Journal of Medicinal Chemistry

Article

Design, Synthesis and Biological Evaluation of Novel, Highly Active Soft ROCK Inhibitors.

Sandro Boland, Arnaud Bourin, Jo Alen, Jacques Geraets, Pieter Schroeders, Karolien Castermans, Nele Kindt, Nicki Boumans, Laura Panitti, Silke Fransen, Jessica Vanormelingen, Jean Marie Stassen, Dirk Leysen, and Olivier Defert

J. Med. Chem., **Just Accepted Manuscript** • Publication Date (Web): 21 Apr 2015

Journal of Medicinal Chemistry is published by the American Chemical Society. 1155 Sixteenth Street N.W., Washington, DC 20036

Design, Synthesis and Biological Evaluation of Novel, Highly Active Soft ROCK Inhibitors.

Sandro Boland, [*,†] *Arnaud Bourin,* [†] *Jo Alen,* [†] *Jacques Geraets,* [†] *Pieter Schroeders,* [†] *Karolien Castermans,* [†] *Nele Kindt,* [†] *Nicki Boumans,* [†] *Laura Panitti,* [†] *Silke Fransen,* [†] *Jessica Vanormelingen,* [†] *Jean Marie Stassen,* [†] *Dirk Leysen* [‡] *and Olivier Defert*[†]

AUTHOR ADDRESS:

[†]Amakem Therapeutics, Agoralaan A bis, 3590 Diepenbeek, Belgium

[‡] CSD Farmakem, Elvire Boelensstraat 7, 9160 Lokeren, Belgium

KEYWORDS: Rho-Kinase, ROCK, SAR, Soft Drug

GRAPHICAL TOC:

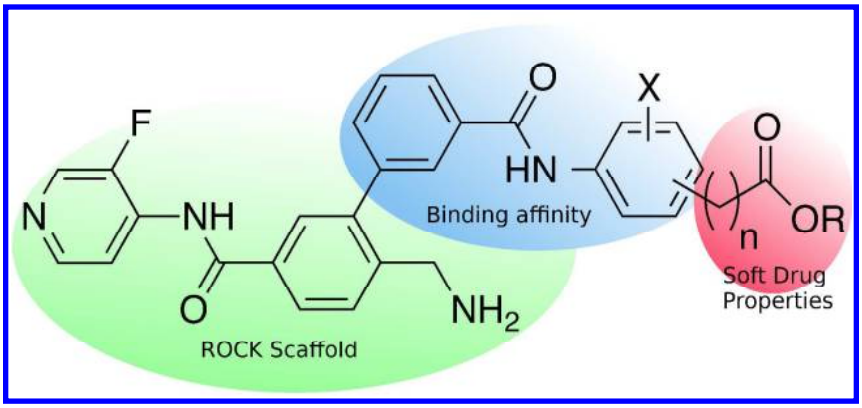

ABSTRACT : ROCK1 and ROCK2 play important roles in numerous cellular functions, including smooth muscle cell contraction, cell proliferation, adhesion and migration. Consequently, ROCK inhibitors are of interest for treating multiple indications including cardiovascular diseases, inflammatory and autoimmune diseases, lung diseases and eye diseases. However, systemic inhibition of ROCK is expected to result in significant side effects. Strategies allowing reduced systemic exposure are therefore of interest. In a continuing effort towards identification of ROCK inhibitors, we here report the design, synthesis and evaluation of novel soft ROCK inhibitors displaying an ester function allowing their rapid inactivation in the systemic circulation. Those compounds display sub-nanomolar activity against ROCK and strong differences of functional activity between parent compounds and expected metabolites. The binding mode of a representative compound was determined experimentally in a single-crystal X-ray diffraction study. Enzymes responsible for inactivation of these compounds once they enter systemic circulation are also discussed.

TEXT:

Introduction

Rho-associated, coiled coil containing protein kinases (ROCKs), also known as Rho-Kinases, are serine/threonine kinases belonging to the AGC family.[1] In humans, ROCKs are represented by two isoforms, namely ROCK1 and ROCK2. These isoforms share an overall homology of 65%, while being 95% homologous in the kinase domain. ROCK plays an important role in numerous cellular processes including smooth muscle cell contraction, cell proliferation, adhesion and migration.[2] Consequently, ROCK inhibitors are of potential interest for the treatment of multiple indications including hypertension,[3] pulmonary arterial hypertension (PAH),[4] inflammatory and autoimmune diseases[5-7] such as asthma, Chronic Obstructive Pulmonary Disease (COPD), Inflammatory Bowel Disease (IBD), and eye diseases[8] (e.g. glaucoma, age-related macular degeneration (AMD)). The ROCK inhibitor Fasudil is used in Japan since 1995 for the treatment of cerebral vasospasm. More recently, Fasudil has shown clinical efficacy on PAH.[9] However, systemic inhibition of ROCK induces a pronounced decrease in blood pressure,[10] and thus reduces the therapeutic window of ROCK inhibitors. Additionally, ROCK inhibitors were recently shown to induce a reversible reduction in lymphocyte counts.[11] As a consequence, systemic ROCK inhibition should preferably be avoided.

Topical application, which results in lower systemic exposure, is a common strategy in the recent development of ROCK inhibitors. The field of eye diseases has received particular attention, and several ROCK inhibitors have been clinically tested as intraocular pressure (IOP)-lowering agents for topical treatment of glaucoma.[8] Those include Y-39983 (Novartis, Basel,

Switzerland), Ripasudil (K-115, Kowa Company Ltd, Nagoya, Japan),[12] AR-12286 & Rhopressa (AR-13324, Aerie Pharmaceuticals, Inc., Bedminster, USA) and ATS907 (Altheos, Inc., South San Francisco, USA). Ripasudil was recently approved in Japan as GLANATEC® ophthalmic solution (0.4%) for the treatment of glaucoma and elevated IOP; and is currently undergoing Phase II trials for treatment of diabetic retinopathy accompanying diabetic macular edema. Additionally, Y-27632, a reference ROCK inhibitor, has delivered promising results with respect to corneal wound healing[13] and several cases of Fuchs corneal dystrophy were successfully treated by administration of Y-27632 eye drops.[14,15] The disclosed structures of some of those ROCK inhibitors are presented in figure 1. Besides ophthalmology, lung diseases were also investigated as potential applications, and ROCK inhibitors optimized towards inhaled delivery and reduced systemic exposure have been proposed for treatment of PAH.[11] Even when used topically, ROCK inhibitors are not devoid of side effects. In the context of ophthalmology, a common adverse event resulting from topical administration of ROCK inhibitors is mild to severe conjunctival hyperemia (redness) due to mechanism-based smooth muscle cell relaxation in conjunctival blood vessels.[8,16,17] Consequently, ROCK inhibitors with an improved therapeutic window would still be of high interest.

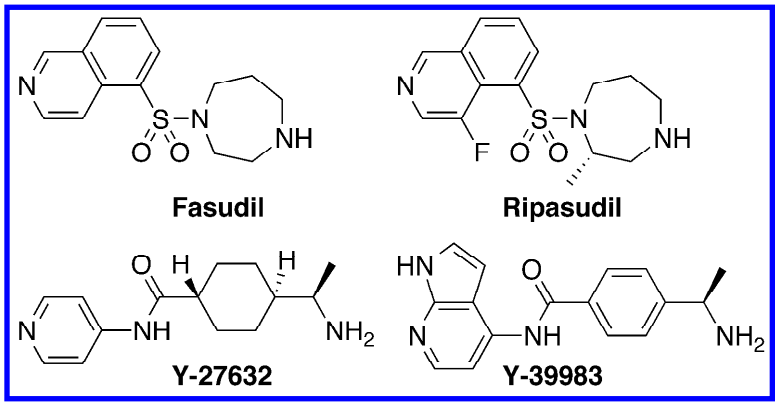

Figure 1. *Structure of the ROCK inhibitors Y-27632, Y-39983, Fasudil and Ripasudil*

Soft drugs are biologically active compounds that are designed to undergo metabolic inactivation by controlled conversion of the parent molecule into a predictable, nontoxic metabolite.[18,19] While soft drugs do not necessarily show fast inactivation, they can be optimized as locally acting compounds, so that they retain sufficient stability in their target organ, while being rapidly inactivated once entering systemic circulation. Such inactivation usually occurs in blood, but can also be achieved in liver. A series of 3-[2-(aminomethyl)-5-[(pyridin-4-yl)carbamoyl]phenyl] benzoates has recently been reported as the first example of soft ROCK inhibitors in literature.[20] As a first proof of concept, **1** (Figure 2) demonstrated *in vivo* effect in rabbits as IOP-lowering agent, without causing noticeable conjunctival hyperemia.[20] Additionally, AMA0076, a soft ROCK inhibitor derived from this series, effectively reduces IOP in ocular normotensive and acute hypertensive rabbits without causing distinct conjunctival hyperemia.[21] This compound has undergone phase IIa clinical trials as an IOP-lowering agent for the treatment of glaucoma. We herein report the design, evaluation and characterization of 4-(aminomethyl)-*N*-(pyridin-4-yl)-3[3-(phenylcarbamoyl)phenyl] benzamide derivatives displaying improved on-target activity and controllable inactivation kinetics.

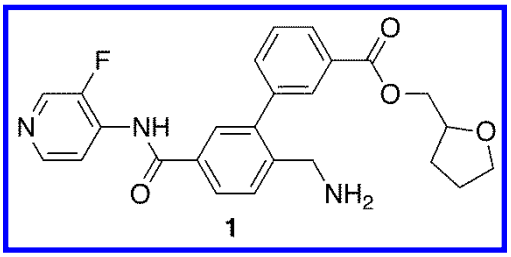

1

Figure 2. *Structure of **1**, a soft ROCK inhibitor with IOP lowering efficacy.*

Results

Our previous work on 3-[2-(aminomethyl)-5-[(pyridin-4-yl)carbamoyl]phenyl] benzoates sought to confer soft drug properties to an existing ROCK inhibitor scaffold. This goal was achieved through the introduction of ester groups that are hydrolyzed in plasma; yielding carboxylic acid metabolites with markedly decreased functional activity.[20] Molecular docking of such ester derivatives inside the ATP-binding site of ROCK1 (Figure 3),[22] however suggested that the on-target activity of this series of compounds could still be improved. Indeed, the newly introduced ester function was positioned in close vicinity of the carboxyl side chain of residue Asp216, potentially causing some degree of electrostatic repulsion. This finding suggested displacement of the ester group towards another part of the scaffold and replacement of the ester by an amide. Additionally, ester derivatives such as **1** had their side chain within contact distance of Phe120. This observation was noteworthy, since Phe120 is present in both ROCK1 and ROCK2, but is absent from all other kinases from the AGC family, with the exception of DMPK (dystrophia myotonica-protein kinase). The simple introduction of an aromatic structure on that position therefore provided the possibility to form specific π-stacking interactions, as well as an opportunity to further increase the selectivity of the chemical series. Combined together, those observations suggested that a benzamide analog such as **2** (Figure 3) could be an interesting platform for the development of further soft ROCK inhibitors, as it would interact favorably with both Asp216 (formation of an additional H-bond) and Phe120 (π-stacking interactions). Interestingly, a number of readily available aniline building blocks display an ester function, thereby offering rapid exploration of structure-activity or structure-property relationships.

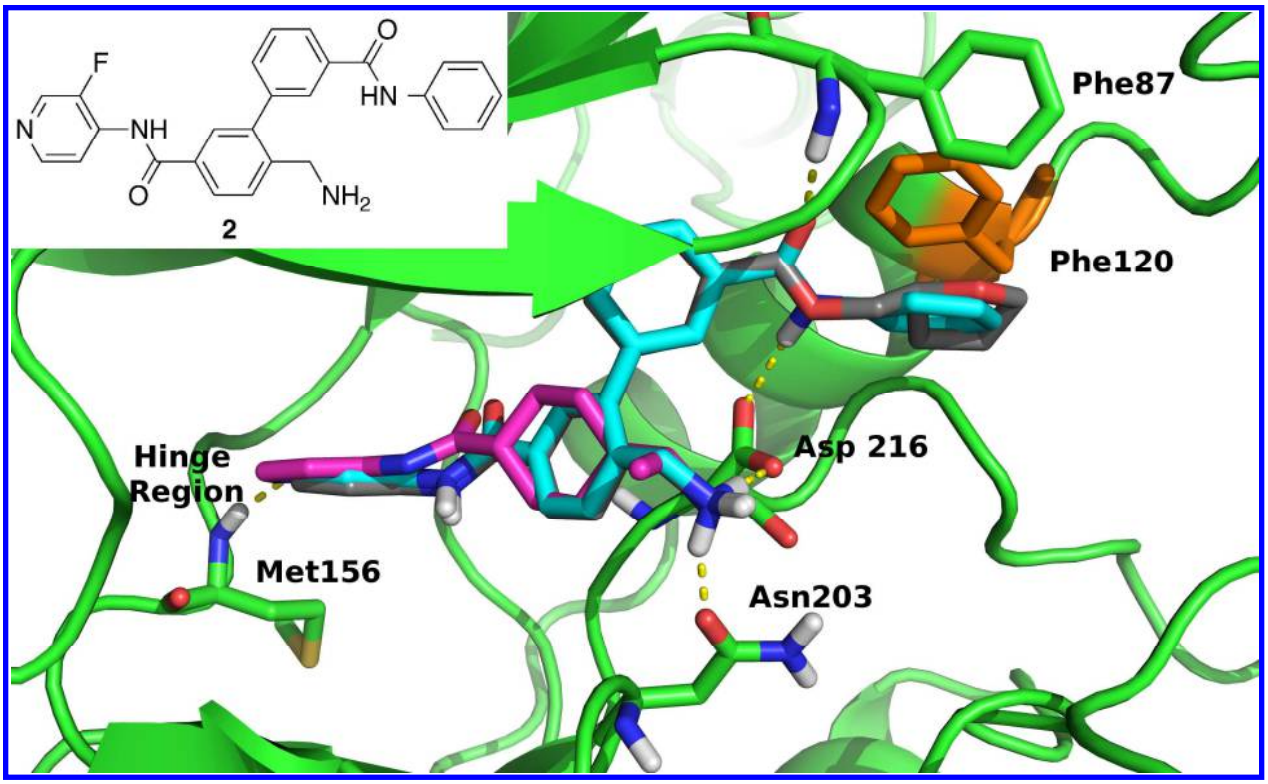

Figure 3. *Molecular modeling of compound* ***1*** *(C in cyan) in the ATP-binding site of ROCK1 (PDB 2ETR; green). The ester function lies in close vicinity (3.8 Å) of the carboxylic acid side chain from Asp216. Additionally, the oxolan-2-yl moiety of* ***1*** *closely contacts the side chain of Phe120 (orange residue). The binding mode suggests replacement of the ester by amide and combination with an aromatic ring to form π-π interactions with Phe120. The resulting structure* ***2*** *is shown in grey. Position of Y-27632 in structure 2ETR is shown for reference (magenta).*

A number of ROCK inhibitors structurally derived from **2** were obtained by adapting the procedure described for the synthesis of earlier soft ROCK inhibitors.[20] Compounds were prepared in *ca.* 3-5 steps, starting from the reported advanced intermediate **3** (Scheme 1).

Scheme 1: *(a) $Pd(dppf)Cl_2$, Na_2CO_3, H_2O, DMF, 100 °C; 16h; (b) T3P, DMAP, DCM, 0°C ➔ rt, 16h; (c) LiOH, ACN/water, rt, 2h; (d) ROH, T3P, DMAP, DCM, 0°C ➔ rt, 16h; (e) HCl(g), DCM, rt, 4h.*

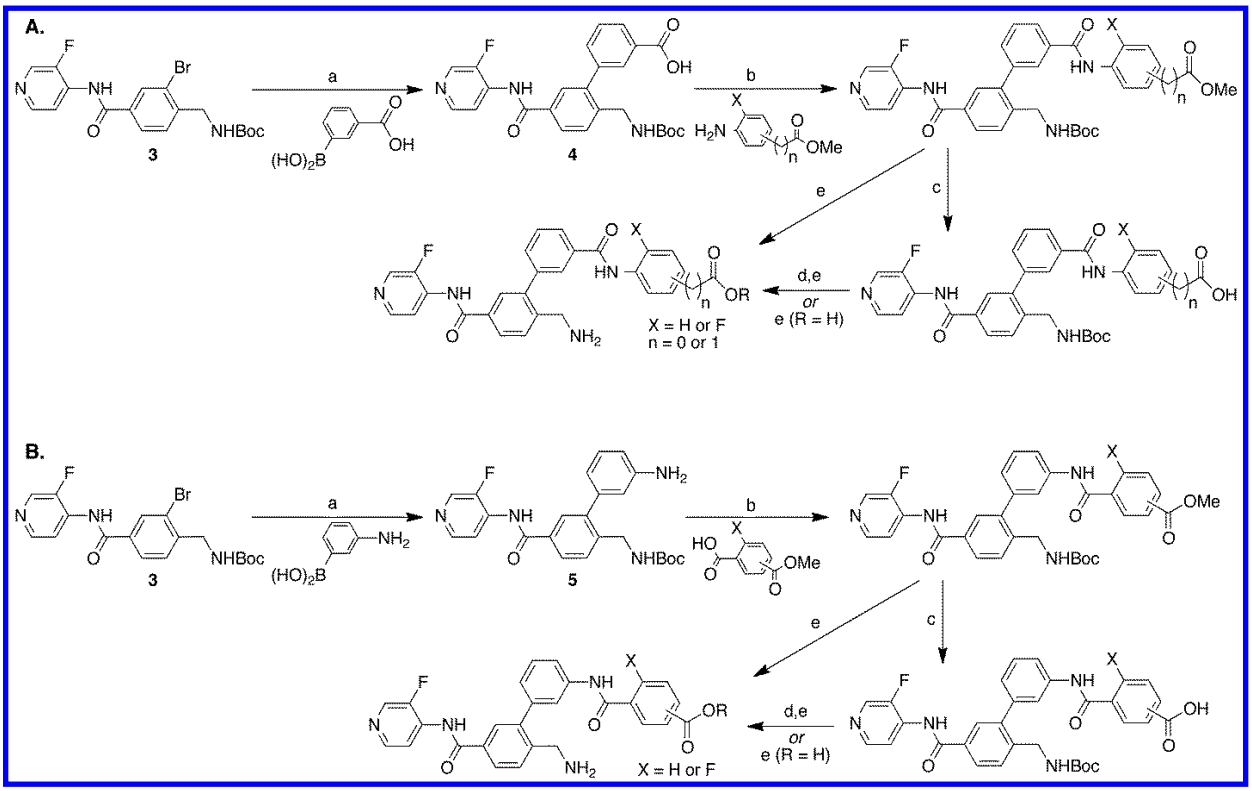

A biphenyl structure, displaying either a carboxylic acid function or an amino function allowing further coupling, is introduced *via* Pd-catalyzed Suzuki reaction, using the commercially available 3-carboxyphenylboronic acid or 3-aminophenylboronic acid, to obtain respectively intermediates **4** and **5**. Amide formation with selected anilines or benzoic acids can be achieved through various methods to activate the acid. T3P used at reduced temperatures proved to be the most effective coupling agent amongst the different conditions tested. At this stage, the intermediate can either be treated with HCl gas, yielding the methyl ester as final compound, or hydrolyzed *via* saponification with 1M aqueous LiOH solution. The resulting carboxylic acid can then be further coupled with various alcohols, allowing modulation of the ester group. As before,

the N-Boc group in the resulting esters is deprotected with HCl gas, to yield the final compounds. Alternatively, the carboxylic acid intermediate can be deprotected and isolated, as this product corresponds to the expected metabolite resulting from enzymatic hydrolysis of the candidate soft ROCK inhibitors.

Table 1. Activity of initial derivatives and corresponding metabolites.

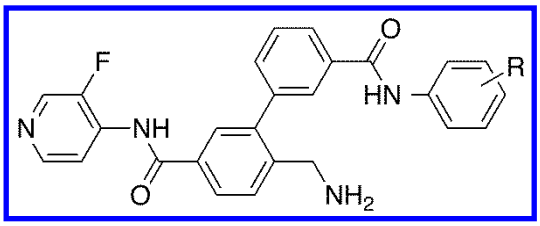

Cpd	R	IC_{50} ROCK1 (nM)	IC_{50} ROCK2 (nM)	IC_{50} ROCK2, 200µM ATP (nM)	EC_{50} MLC-PP (nM)[a]	$t_{1/2}$ Plasma (min)[b]
Y-27632	NA	NT	54 ± 16	NT	630	>120
Ripasudil	NA	NT	3.8 ± 1.4	197 ± 50	210	NT
1	NA	NT	2.5 ± 0.5	49 ± 16	94	<5
2	H	NT	<1	31 ± 8	22	>120
6	3-CO_2Me	<1	1.1 ± 0.5	125 ± 18	79	<5
7	3-CH_2CO_2Me	<1	1.1 ± 0.5	144 ± 56	220	<5
8	4-CO_2Me	<1	<1	4.1 ± 1.0	3.0	>120
9	4-CH_2CO_2Me	<1	<1	11 ± 2	31	<5
6M	3-CO_2H	NT	6.6 ± 0.6	NT	5900	>120
7M	3-CH_2CO_2H	NT	1.5 ± 0.5	NT	1300	>120
8M	4-CO_2H	NT	3.3 ± 0.8	NT	6600	>120
9M	4-CH_2CO_2H	NT	1.8 ± 0.6	NT	3600	>120

[a]: Mean of at least 3 exp. [b]: Mean of at least 2 exp. NA: Not applicable. NT: Not tested.

Firstly, we evaluated **2**, our generic template used for the development of additional soft ROCK inhibitors, in a radiometric assay measuring phosphorylation of a peptidic substrate.[23] This compound encouragingly displayed a sub-nanomolar IC_{50} value under standard assay conditions, which involve presence of 1 nM enzyme and 1 μM ^{32}P-ATP. Such activity was superior to Ripasudil and largely superior to Y-27632. While Y-27632 appeared relatively potent in this assay (54 nM) compared to literature data (IC_{50} 100-200 nM), its activity remained consistent throughout independent experiments. One reason behind this observation could be the low ATP concentration, which is under K_m and favors lower IC_{50} values. The encouraging potency of **2** was confirmed by strong functional activity in the myosin light chain phosphorylation (MLC-PP) assay.[24] Compound **2** also displayed high stability in human plasma (>90% remaining after 2 h). Consequently, hydrolysis of the added ester function should be considered the only plausible mechanism of inactivation in plasma for upcoming soft drug candidates. Addition of simple methyl esters on positions 3 and 4 was tolerated and yielded compounds **6-9**, which all displayed low-nanomolar or sub-nanomolar activity against both ROCK1 and ROCK2 (Table 1). As the measured IC_{50} values were similar to or lower than formal ROCK concentration (1 nM), comparison under standard assay conditions was actually judged unreliable. However, as compounds were designed to occupy the ATP-binding site of ROCK, we reasoned that the inhibition they cause would be competitive with respect to ATP. A follow-up experiment was therefore carried out in presence of higher ATP concentration (200 μM) to reduce apparent inhibition and provide a more useful comparison. As expected, a clear IC_{50} shift was observed for most compounds, confirming their ATP-competitive behavior. The resulting data indicated that substitution on position 4 yielded stronger ROCK inhibitors, as both **8** and **9** improved over **1** and **2**. Most notably, **8** retained an impressive IC_{50} of 4 nM when facing

the increased ATP concentration. On the other hand, **6** and **7** displayed a moderate loss of activity (4 to 5-fold) with respect to **2**. Evaluation in presence of 200 μM ATP was also more in line with the functional EC_{50} values observed in the MLC-PP, with **8** and **9** inducing the strongest inhibition of MLC phosphorylation and appearing more active than Y-27632 or Ripasudil. Stability in human plasma further differentiated **8** from the other ester derivatives, as the former had $t_{1/2}$ > 120 min, while the latter were all degraded within minutes.

The carboxylic acids resulting from ester hydrolysis, which represent the expected metabolites of compounds **6-9**, were also evaluated. While those acids retained single digit nanomolar activity in the enzymatic ROCK2 assay, they nonetheless displayed a significant decrease of functional activity in the MLC-PP assay, thereby validating ester hydrolysis as a viable inactivation mechanism for the design of soft ROCK inhibitors. This loss of activity could be attributed, to some extent, to reduced membrane permeability of the metabolites, as can be seen by comparing **8** and **8M** (Table 2). This difference is understandable,[25] as metabolites, which are zwitterions at physiological pH, display decreased lipophilicity and increased topological polar surface area (TPSA) compared to their parent compounds. In this respect, it should be noted that **8** already displayed reduced permeability compared to **2**, possibly because of its already increased TPSA. After evaluation of this first group of analogs, we had therefore identified potent ROCK inhibitors displaying different profiles, which prompted us for the optimization of **6**, **8** and **9** as separate sub-series. **7** was not subjected to further optimization, in view of the weaker inhibition of ROCK2 (IC_{50}) in presence of 200 μM ATP, of the lower functional activity (EC_{50}), and of the smaller differences between parent compound and carboxylic acid metabolite.

Table 2. Caco-2 permeability, logD and TPSA for selected compounds

	Caco-2 P_{app} (10^{-6} cm s^{-1})[a]	logD (pH 7.4)[b]	TPSA (Å²)
2	2.3	1.96*	99
8	0.8	2.74 (exp) /1.97*	125
8M	0.08	-0.56 (exp) /1.20*	139

*[a]: Mean of two experiments. [b]: Mean of 3 experiments. *: Calculated (Instant J. Chem 6.3.3);*

The aim of optimization of compound **6** was to increase functional activity while modulating its stability. Indeed, while rapid inactivation in plasma is *per se* of interest for soft drug design, the possibility of modulating compound stability according to the needs of a specific application or target organ is also of high value. The hydrolysis rate of an ester by esterases such as acetylcholinesterase is known to be the combined result of intrinsic compound reactivity, affinity for the esterase and catalytic efficiency for a particular ester,[26] and those combined factors can potentially be used to modulate compound softness. In order to explore structure-activity and structure-property relationships, we first opted for modification of the amide linker, modification of the ester side chain, and introduction of fluorine on the benzoic acid moiety (Table 3). The corresponding metabolites were also synthesized.

Several of the resulting compounds were very strong ROCK2 inhibitors and, as discussed above, could only be differentiated when evaluated against a higher ATP concentration. Increasing the size of the alkyl chain was at best tolerated (**6** *vs.* **12**), but led in some occasions to a drop in on-target activity (**6** *vs.* **11**). Those observations were consistent with the MLC-PP assay, as compounds with the highest on-target activity tended to have the highest effect on MLC phosphorylation. Variation of ester moiety had a drastic effect on stability in human plasma.

Table 3. Structure-activity and structure-property relationships for analogs of **6** and their corresponding metabolites.

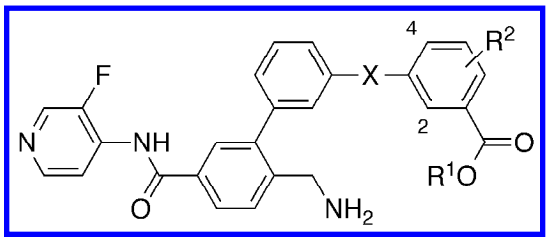

Cpd	R^1	R^2	X	IC_{50} ROCK2 (nM)	IC_{50} ROCK2, 200μM ATP (nM)	EC_{50} MLC-PP (nM)[a]	$t_{1/2}$ Plasma (min)[b]	Expected Metabolite
6	Me	H	C=ONH	1.1 ± 0.5	125 ± 18	79	<5	**6M**
10	i-Pr	H	C=ONH	7.0 ± 0.6	NT	150	34	**6M**
11	n-But	H	C=ONH	27 ± 12	NT	180	<5	**6M**
12	sec-But	H	C=ONH	2.6 ± 0.5	NT	77	16	**6M**
13	Me	4-F	C=ONH	1.6 ± 0.6	46 ± 12	26	18	**13M**
14	n-Pr	4-F	C=ONH	2.1 ± 0.5	NT	75	<5	**13M**
15	(S) sec-But	4-F	C=ONH	5.5 ± 0.6	72 ± 17	50	39	**13M**
16	(R) sec-But	4-F	C=ONH	3.3 ± 0.5	NT	79	46	**13M**
17	Me	H	NHC(=O)	<1	2.1± 0.8	17	64	**17M**
18	n-Pr	H	NHC(=O)	1.8 ± 0.5	NT	15	<5	**17M**
19	Me	4-F	NHC(=O)	<1	1.4 ± 0.9	6.8	53	**19M**
20	$(CH_2)_2OMe$	4-F	NHC(=O)	<1	2.2 ± 1.4	26	<5	**19M**
21	Me	2-F	C=ONH	1.2 ± 0.5	8.8 ± 2.1	11	<5	**21M**
22	cPen	2-F	C=ONH	1.4 ± 0.5	41 ± 14	43	9	**21M**
6M	H	H	C=ONH	6.6 ± 0.6	NT	5900	>120	NA
13M	H	4-F	C=ONH	2.0 ± 0.6	NT	3900	>120	NA
17M	H	H	NHC(=O)	<1	NT	2000	>120	NA
19M	H	4-F	NHC(=O)	<1	NT	8900	>120	NA
21M	H	2-F	C=ONH	3.5 ± 0.7	NT	>10000[c]	>120	NA

[a]: Mean of at least 3 exp. [b]: Mean of at least 2 exp. [c] Highest tested concentration. NA: Not applicable. NT: Not tested.

Replacement of a methyl ester by n-propyl ester resulted in substantially faster degradation (**13** *vs.* **14** or **17** *vs.* **18**). Esters synthesized from secondary alcohols were of particular interest for modulating stability. Indeed, the isopropyl ester **10** initially led to a significant increase of plasma stability. However, further enlargement of this group towards *sec*-butyl ester (**12**)

resulted in faster degradation. In 2-F or 4-F series, *sec*-butyl esters (**15**, **16**) or cycloalkyl esters (**22**) were also hydrolyzed in plasma. Reversal of the amide linker resulted in increased activity, but also in increased stability (**6** *vs.* **17**; **13** *vs.* **19**). The latter could again be easily varied by changing the ester chain (**18**, **20**). Fluorine atoms allowed further modulation of activity and plasma stability (e.g. **6** *vs.* **13** or **21**), depending on their position and on the amide linker that was used.

Ultimately, this optimization exercise allowed the identification of derivatives displaying improved cellular activity and covering a range of plasma stabilities. As examples, **17**, **19** and **21** all displayed EC_{50} values under 20 nM, while their plasma $t_{1/2}$ ranged from >60 min to <5 min.

At this point, we sought to experimentally verify the binding mode of soft ROCK inhibitors in ROCK, so to provide further rationale for the observed SAR and additional insights regarding compound optimization. Several soft ROCK inhibitors, including **8** and **13**, were selected for crystal soaking, based on their on-target potency, cell-based activity and sufficient solubility. The best ROCK2 co-crystals were obtained with compound **13**, allowing XRD data collection at a resolution of 2.93 Å. In the resulting structure (Figure 4), ROCK2 adopts a bilobal architecture characteristic of other members of the eukaryotic protein kinase family. As seen in other crystal structures of ROCK1 and ROCK2, the protein crystallized as a dimer,[22] with four monomers in the asymmetric unit. The amino acid residues forming the active (ATP-binding) site and the ligand were well defined in the electron density map. The interpreted X-ray diffraction data shows a clear binding mode, as well as the orientation and conformation of the bound ligand. In line with our expectations, the part of the inhibitor that is similar to Y-27632 occupies the ATP-binding site in a fashion that is almost identical to this reference compound. The additional structural elements of **13** however form numerous interactions which contribute to the increased

on-target activity. The biphenyl structure that was already present in previous soft ROCK inhibitors sits under the P-loop (Glycine-rich loop) and forms a π-cation interaction with Lys121. Comparison to the crystal structure of a ROCK1-Y-27632 complex (2ETR),[22] reveals that the increased bulkiness of **13** did not result in a repulsion of the P-loop, that instead moved in direction of the inhibitor, forming additional contacts. As intended, the additional benzamide structure engages the side chains of Phe103 and Phe136 in π-stacking interactions. Based on a distance of 3.5 Å between donor and acceptor, a total of six hydrogen bonds are observed between ROCK2 and **13**. In addition to the hydrogen bonds already observed in the ROCK1-Y-27632 complex,[22] the newly introduced carbamoyl function forms two hydrogen bonds with residues Phe103 and Asp232, as suggested by molecular modeling studies. The last hydrogen bond involves the ester carbonyl and the side chain of Thr235, in three of the four ROCK2 monomers present in the unit cell. However, the benefits of such an interaction are probably lessened by electrostatic repulsion with the neighboring side chain of Asp214. This observation might explain why esters on position 4 display stronger on-target activity than on position 3. While the methyl ester of **13** appears to take a slightly different conformation depending on the monomers, position of the terminal methyl group is not clearly defined. In all cases, this ester nonetheless sits in a region that is solvent-exposed, explaining why further addition of hydrophobic side chains does not result in improved activity.

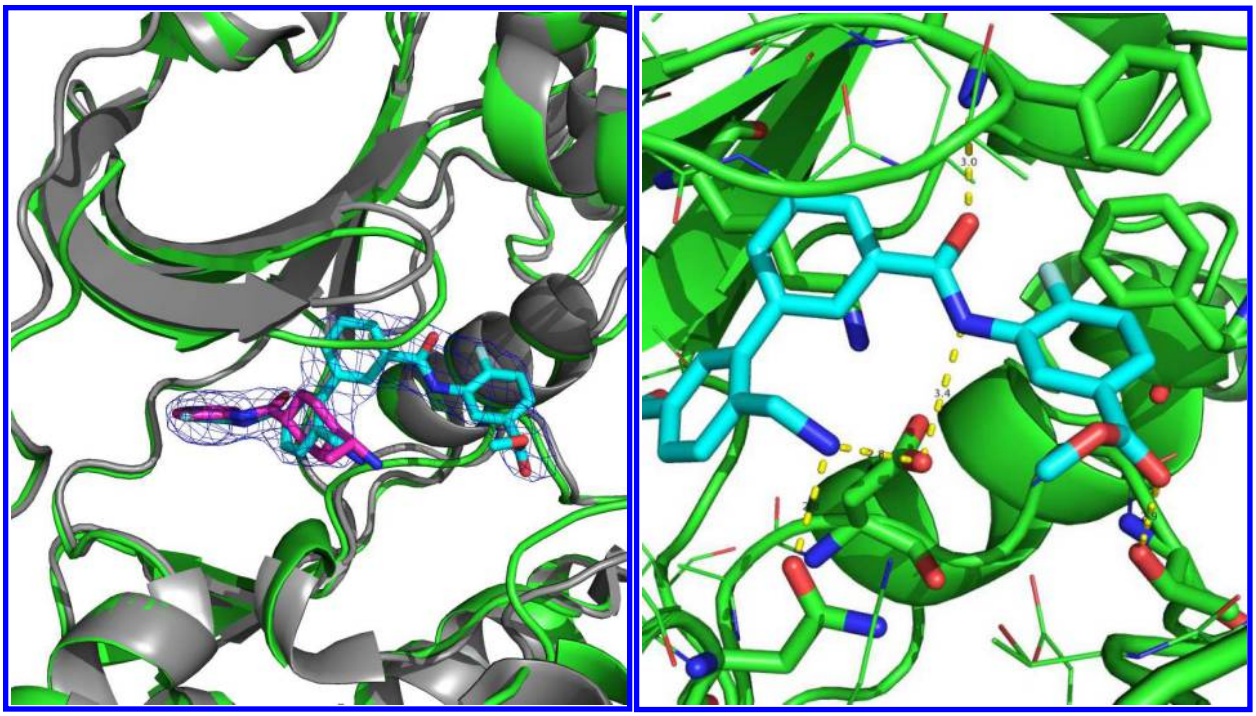

Figure 4. *Crystal structure of a complex between ROCK2 and* ***13****. A) Comparison of the ROCK2-****13*** *(protein in green,* ***13*** *in cyan) and ROCK1-Y-27632 (protein in grey, compound in magenta) complexes. Movement of the P-loop above the arylamide structure is visible. B) Focus on the newly added structural elements, and on the additional hydrogen bonds formed by* ***13****.*

Optimization of **9** focused on modulation of the stability profile *via* introduction of secondary alcohols, since the starting compound already possessed strong on-target activity and functional activity (Table 4). In contrast to the analogs of **6**, several derivatives with larger alcohol chains such as **24-26** or **29**, retained sub-nanomolar IC_{50} values, even when facing a higher ATP concentration. Activity in the MLC-PP assay was however reduced by the presence of polar functions, as demonstrated by **30** (N-methyl-piperidin-4-yl). As for carboxylic acid metabolites, this weaker EC_{50} value likely results from lower membrane permeability. As observed with analogs of **6**, plasma stability was initially increased for esters from secondary alcohols (**23)**, but decreased once cyclic alcohols were used (**26-30)**. Interestingly, we noted a significant difference

of plasma stability between **24** and **25**, the (S) and (R) enantiomers of the sec-butyl ester, while chirality did not affect the hydrolysis of **15** and **16**.

Table 4. Structure-activity relationships for analogs of **9** and their common metabolite.

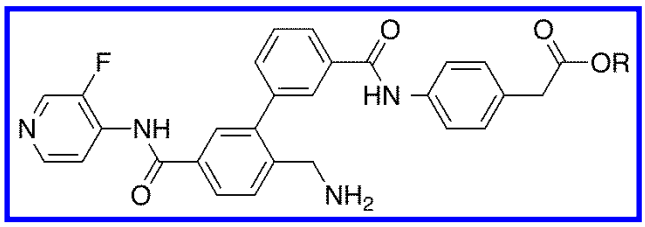

Cpd	R	IC_{50} ROCK2 (nM)	IC_{50} ROCK2, 200μM ATP (nM)	EC_{50} MLC-PP (nM)[a]	$t_{1/2}$ Plasma (min)[b]	Expected Metabolite
9	Me	<1	11 ± 2	31	<5	**9M**
23	i-Pr	<1	<1	37	94	**9M**
24	(S) sec-But	<1	<1	23	17	**9M**
25	(R) sec-But	<1	<1	31	>120	**9M**
26	THP-4-yl	<1	<1	79	7	**9M**
27	c-But	1.3 ± 0.5	1.4 ± 0.6	24	6	**9M**
28	c-Pen	<1	1.3 ± 0.6	26	7	**9M**
29	THP-3-yl	<1	<1	36	6	**9M**
30	N-Me-piperidin-4-yl	<1	4.6± 1.9	330	<5	**9M**
9M	H	1.8 ± 0.6	NT	3600	>120	NA

[a]: Mean of at least 3 exp. [b]: Mean of at least 2 exp. NA: Not applicable. NT: Not tested.

In view of the observed differences in plasma stability, we sought to characterize the enzyme(s) responsible for hydrolysis of the soft ROCK inhibitors in systemic circulation. Therefore, we assessed the effect of various esterase inhibitors on hydrolysis rate (Figure 5). In a first step **13**

was incubated in human whole blood in presence of DTNB (arylesterase inhibitor), EDTA (PON1 inhibitor), PMSF (generic serine protease / serine esterase inhibitor), BNPP (carboxylesterase inhibitor) or tacrine (cholinesterase inhibitor). BNPP had no effect on the hydrolysis rate of **13**, consistent with literature indicating little or no carboxylesterase activity in human plasma.[27] DTNB and EDTA did not significantly alter the hydrolysis rate of **13** either. This finding is in line with the absence of aryl ester or lactone, which represent the preferred substrates of those enzymes,[28] in **13**. In opposition, addition of PMSF or tacrine both prevented any significant degradation of **13** over the course of the experiment (120 min), suggesting that cholinesterase activity is responsible for the hydrolysis of **13**. In a second step, the effect of tacrine on the stability of additional derivatives of **6** and **9** spanning a range of hydrolysis rates ($t_{1/2}$ in human plasma from <5 min to 53 min) was assessed by measuring the residual amount of compound after 60 min incubation. We observed that addition of 5 μM tacrine was sufficient to completely prevent hydrolysis of all but the most labile derivatives. The minor degradation that is still found for **20** and **26** was attributed to the residual cholinesterase activity still present at this inhibitor concentration, as the limited time of the experiment does not allow significant chemical hydrolysis.

Optimization of **8** was initially limited to a small number of derivatives, in an attempt to determine if plasma stability could be modulated. While they maintained on-target (ROCK2), and functional (MLC-PP) activity, introduction of *n*-propyl ester **(31)** or reversal of the amide linker **(32)** did not result in faster degradation in human plasma (Table 5).

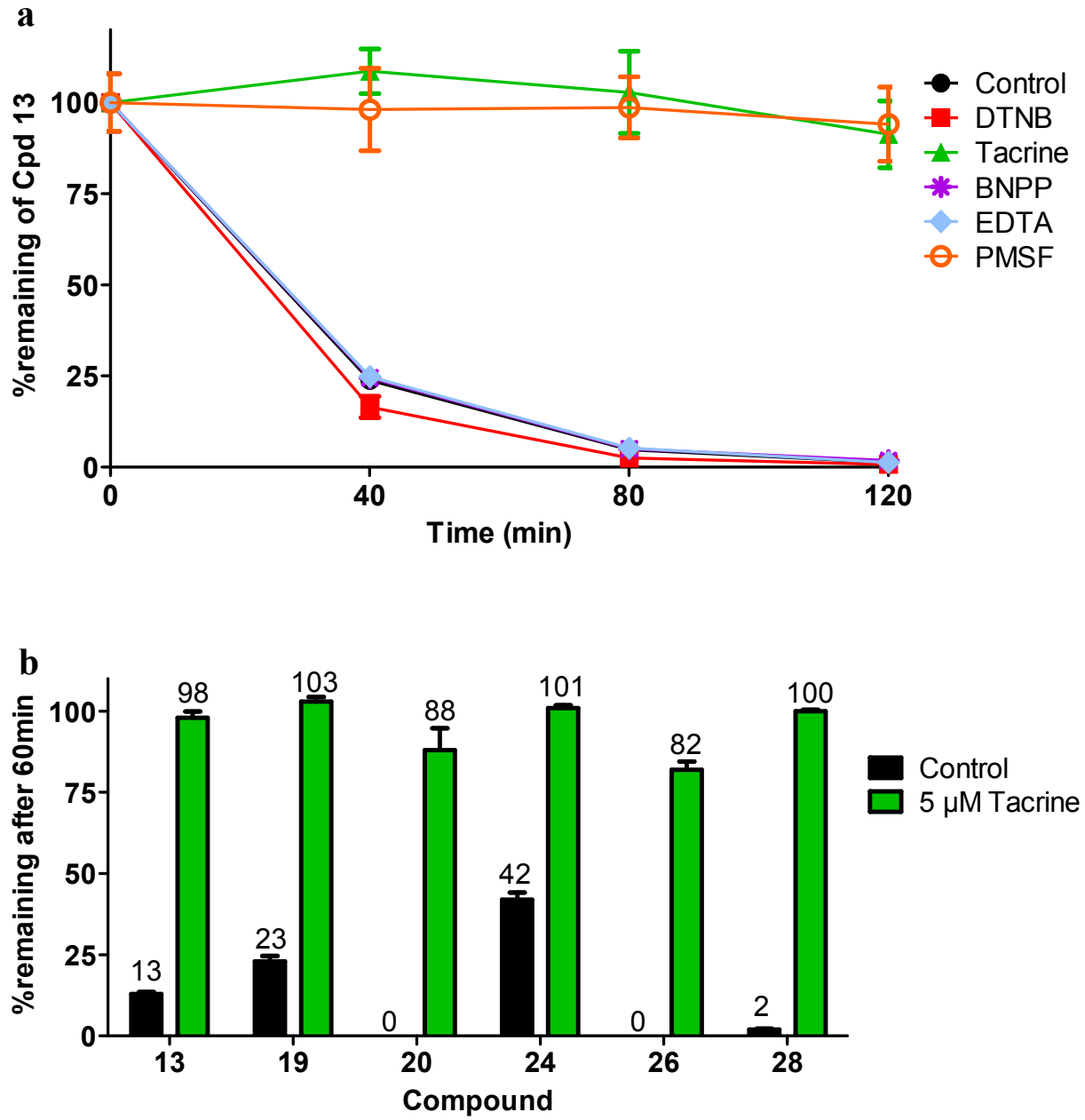

Figure 5. *a) Effect of five esterase inhibitors on the hydrolysis rate of* ***13*** *in human whole blood.*

b) Effect of tacrine on the hydrolysis rate of selected soft ROCK inhibitors in human plasma.

Table 5. Structure-activity relationships for analogs of **8** and the corresponding metabolites.

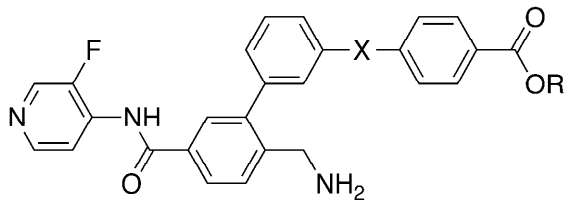

Cpd	R	X	IC_{50} ROCK2 (nM)	IC_{50} ROCK2, 200µM ATP (nM)	EC_{50} MLC-PP (nM)[a]	$t_{1/2}$ Plasma (min)[b]	Expected Metabolite
8	Me	C=ONH	<1	4.1 ± 1.0	3.0	>120	**8M**
31	*n*-Pr	C=ONH	<1	NT	8.3	>120	**8M**
32	Me	NHC(=O)	<1	3.1 ± 1.1	5.2	>120	**32M**
8M	H	C=ONH	3.3 ± 0.9	NT	6600	NT	NA
32M	H	C=ONH	1	NT	3600	NT	NA

[a]: Mean of at least 3 exp. [b]: Mean of at least 2 exp. NA: Not applicable. NT: Not tested.

Being faced with the high stability of those derivatives in plasma, we reasoned their conversion to the carboxylic acid metabolite might still occur in liver. Indeed, liver tissue has high esterase activity, resulting from the presence of carboxylesterase 1 (CES1, also known as liver carboxylesterase) and to a lesser extent carboxylesterase 2 (CES2), which are both absent from human plasma. In order to validate that hypothesis, the stability of **8** in presence of human or rabbit (New Zealand White, NZW) hepatocytes was first investigated. As expected, **8** was rapidly degraded ($t_{1/2}$=12 min for both human and rabbit hepatocytes) under the tested conditions, with only limited compound (2.4% ± 1.3% in human hepatocytes, 0.4% ± 0.3% in rabbit hepatocytes) remaining after 120 min of incubation. In the meantime, the formation of an equivalent amount of **8M** (corresponding to 99.3 ± 0.8 % of the parent compound in human hepatocytes) was observed, confirming that **8** is degraded through ester hydrolysis.

Table 6. Pharmacokinetic data for **8**

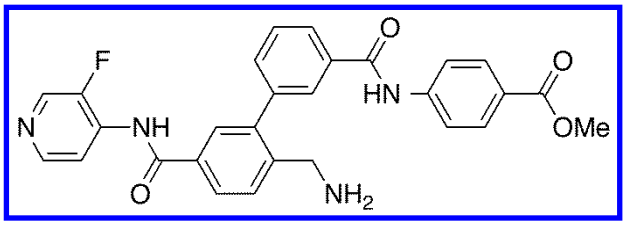

Parameter	Study	Value
$t_{1/2}$ human plasma	Plasma incub.	> 120 min
$t_{1/2}$ rabbit plasma	Plasma incub.	> 120 min
$t_{1/2}$ vs. human hepatocytes	Hepatocyte incub.	12 min
$t_{1/2}$ vs. rabbit hepatocytes	Hepatocyte incub.	12 min
Plasma C_{max} for **8** (iv, rabbit, 0.1 mg/kg)	Rabbit PK	803 nM (1 min)
Plasma C_{max} for **8M**	Rabbit PK	255 nM (10 min)
AUC_{last} for **8** (iv, rabbit, 0.1 mg/kg)	Rabbit PK	5090 nM min
AUC_{last} for **8M**	Rabbit PK	21500 nM min

As a next step, **8** was submitted to a pharmacokinetic study in rabbit. Firstly, we confirmed that **8** was essentially as stable in rabbit plasma as in human plasma ($t_{1/2}$ > 120 min). NZW rabbits received **8** intravenously (0.1 mg/kg) and plasma samples were taken at time points ranging from 1 to 360 minutes after administration. The resulting pharmacokinetic parameters are summarized in table 6. The concentration of **8** was highest for the 1 min time point (803 ± 218 nM) and was markedly reduced at the 5 min and 10 min time points (176 ± 18 nM and 57 ± 1 nM respectively). A slower, but still rapid decay ($t_{1/2}$ = 22 min) was subsequently observed. **8** remained above level of quantitation (8 nM) until the 30-60 min time points. Formation of **8M** was already apparent at the 1 min time point, and plasma concentration of **8M** was highest (255

nM ± 34 nM) after 10 min. **8M** remained above level of quantitation (35 nM) until the 120 min time point and was still detectable after 240 min. In view of the rapid elimination of **8** and of the concomitant formation of **8M**, we considered that an equilibrium in plasma / tissue distribution of **8** could not be reached in this experiment. The distribution volume and clearance parameters were therefore not calculated. From a soft drug perspective, the collected data nonetheless demonstrate *in vivo* formation of the expected carboxylic acid metabolite and higher (4.2-fold) exposure for **8M** than for **8**. Thus, we concluded that derivatives displaying the ester moiety on position *para*, such as **8**, can qualify as soft drugs, in spite of their apparent stability in plasma.

The selectivity of **8** was investigated against a panel of 335 kinases (Reaction Biology Corp). Compound was tested at 10 nM and 100 nM, against an ATP concentration of 10 μM, with the highest levels of inhibition found for ROCK1 and ROCK2. A selectivity score was attributed to **8** by calculating the fraction of "off-target" kinases that are hit (>50% inhibition) at the tested concentration, in a fashion similar to Karaman *et al.* (Ambit selectivity score).[29] The $S_{(100\ nM)}$ for **8** was 0.045. This score should be put in perspective with the sub-nanomolar IC_{50} of **8** against ROCK, and reflects selectivity of at least 100-fold *vs.* other kinases. Most of the off-target activities identified at 100 nM were located within the AGC kinase family, with the strongest inhibition being found for novel PKCs (PKCε, PKCη, PKCδ and PKCθ), MSK1, PRK1, PRK2 and PRKX. Interestingly, PRK2 mediates some of the cellular effects of the reference ROCK inhibitors Y-27632[30] and Fasudil,[31] suggesting that this "off-target" activity might actually be beneficial. The $S_{(10\ nM)}$ score of **8** was 0.006. This score is more in line with the criterion of a 10-fold ratio between K_d values that was initially defined by Karaman *et al.*, and positions **8** as a nicely selective ROCK inhibitor. PKCη and PRK2 were, besides ROCKs, the only kinases inhibited (> 50%) targeted in presence of 10 nM of **8**.When tested in the same panel, **8M**

displayed a $S_{(100\ nM)}$ score of 0.012, and did not inhibit any kinase that wasn't previously affected by **8**. The off-target activities of **8M** were in general weaker, with the exception of MSK1 & 2. Results from the selectivity panel are illustrated in Figure 6.

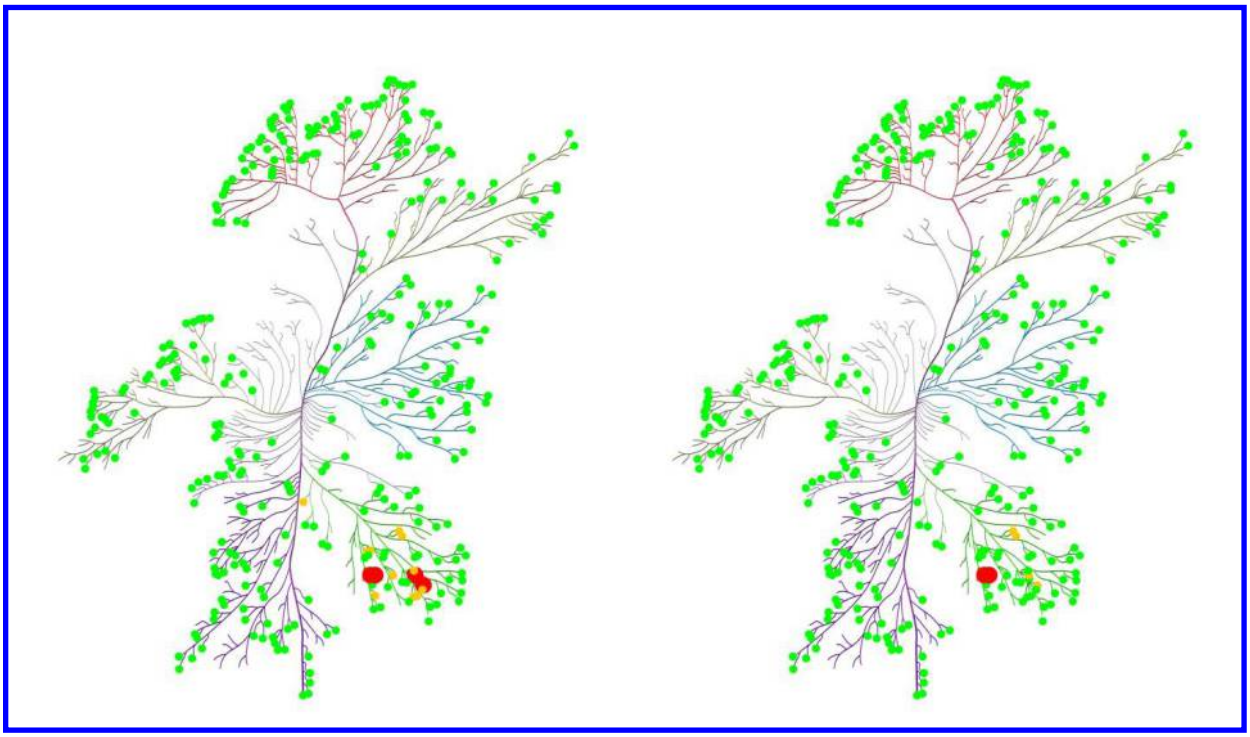

Figure 6. *Kinase selectivity data for* ***8*** *(left) and* ***8M*** *(right). Both compounds were tested at a concentration of 100 nM, against 10 μM ATP. Red dots denote >90% inhibition of kinase activity, while orange dots indicate 50-90% inhibition. Figure drawn with Kinase Mapper (Reaction Biology Corporation).*

In addition to MLC phosphorylation, selected soft ROCK inhibitors were evaluated in further cell-based assays. Rho and ROCK play key roles in cell migration and motility.[2] ROCK inhibition by Y-27632 was shown to increase migration of several cell lines, including T3T fibroblast, human tenon fibroblasts (HTF) or epithelial (T84, Caco-2) cell lines.[30,32] Among others, we chose to follow migration of human dermal fibroblast (HDF-1) cells as a measure for

cellular functional activity of the soft ROCK inhibitors, in an in-house implemented wound assay previously used on vascular endothelial cell lines.[33] In a first step, cytotoxic effects on the HDF-1 cell line were assessed using both a viability assay (WST-1) and apoptosis assay (Caspase-3/7 induction). The cytotoxic concentration 50 (CC_{50}), corresponding to a 50% decrease in viability after 24h, was 46 μM for **8**, 45μM for **13** and 29 μM for **28**. Such values are in line with the induction of apoptosis in the HDF-1 cells by those compounds. Indeed, **8** and **13** both showed a significant induction of caspase 3/7 activity as of 60 μM (24 h treatment), while induction of apoptosis could be observed as of 40 μM for **28** (significant at 100 μM). In a second step, migration of HDF-1 was followed for 8 h, in presence of non-cytotoxic concentrations of the ROCK inhibitors. **8**, **13** and **28** all increased cell migration of the HDF-1 in a concentration dependent manner, as compared to the equivalent DMSO controls after wounding of the monolayer (Figure 7). **8** was most efficient, since significantly increased migration was observed as of 0.001 μM (Figure 7A). **13** showed an induction of migration as of 0.01 μM whereas **28** only significantly stimulated migration at 0.1 μM (Figures 7C & 7D). The corresponding metabolites did not display significant effects on cell migration until at least 1 μM (illustrated for **8M**, Figure 7), in line with their lower activity in MLC-PP assay. Similar data could be collected over additional cell lines, prompting the evaluation of compounds in *in vivo* preclinical models of corneal wound healing[34] or AMD.[35] Those results are discussed in separate dedicated papers.

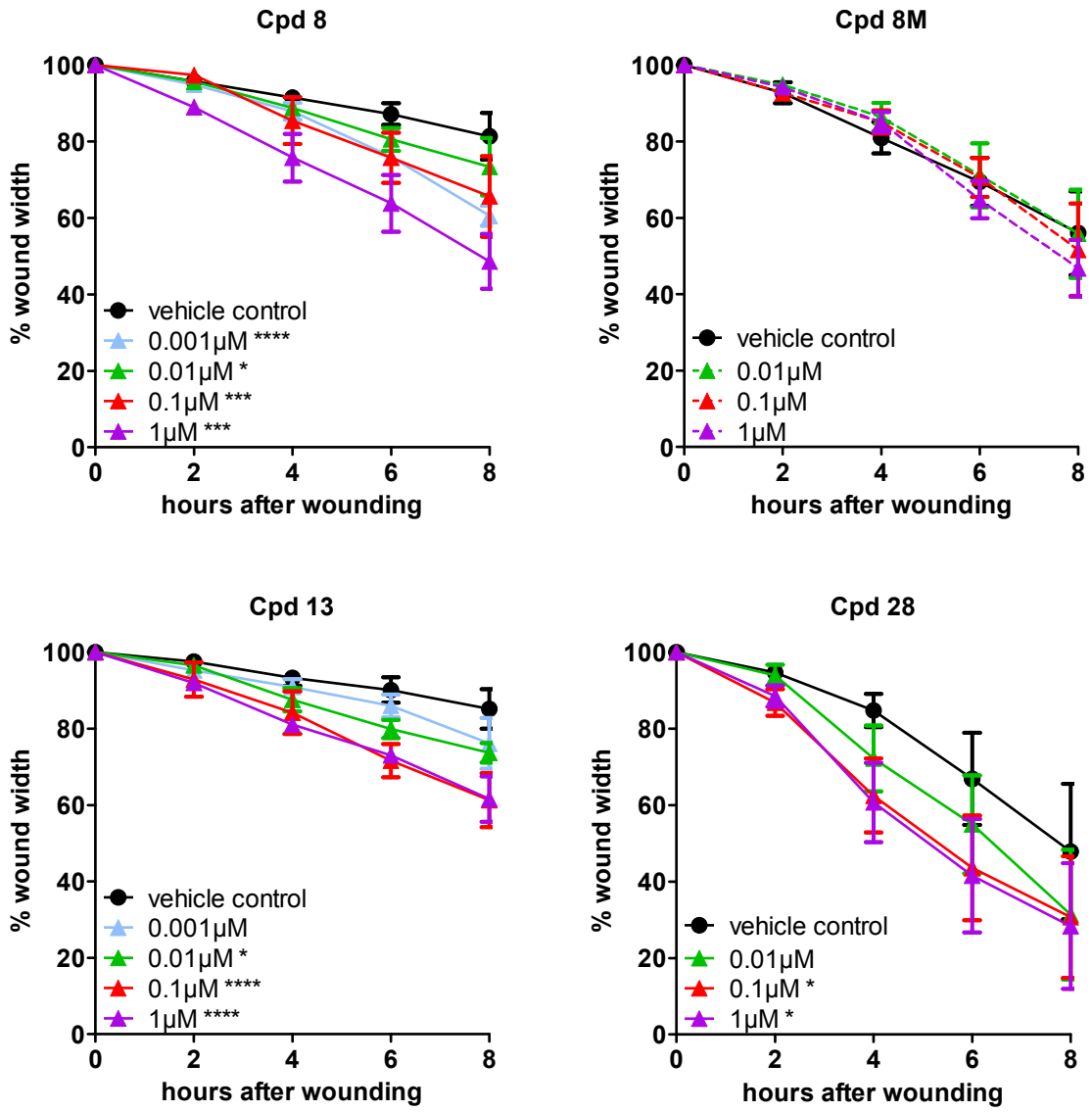

Figure 7. *Effect of* ***8****,* ***8M, 13*** *and* ***28*** *in a HDF-1 migration assay. All three parent compounds show a dose-dependent effect on migration, which is significant with respect to vehicle as of 0.001 µM (****8****), 0.01 µM (****13****) or 0.1 µM (****28****). In contrast,* ***8M*** *does not differ from the vehicle control at 0.01, 0.1 or 1 µM.*

Discussion:

For several years, ROCK has been identified as a potentially attractive target for the treatment of multiple indications including cardiovascular diseases,[3] inflammatory and autoimmune diseases,[5-7] and eye diseases.[8] Unfortunately, the potent effect of ROCK inhibitors on blood pressure has hampered their development for indications where systemic exposure is either required or likely. Consequently, development of ROCK inhibitors was often focused on topical applications resulting in low systemic exposure, with the field of eye diseases receiving particular attention. Even so, the side effects of locally applied ROCK inhibitors (e.g. conjunctival hyperemia in case of administration as eye drops) remain a matter of debate. In this context, soft drugs represent an attractive approach for minimizing ROCK-associated side effects, by reducing systemic exposure to ROCK inhibitors.

While our previous work started with the introduction of an ester moiety onto an existing scaffold, we here sought to optimize the on-target and functional activity of our ROCK inhibitor series. Our efforts were largely successful, as the resulting compounds stand among the strongest ROCK inhibitors reported to date, retaining low nanomolar IC_{50} values even when facing high ATP concentrations. Moreover, activity in a cell-based MLC phosphorylation assay was demonstrated, and an important difference of functional activity was observed between the parent compounds and their carboxylic acid metabolites, thereby validating ester hydrolysis as a viable strategy for the design of soft ROCK inhibitors. In spite of those achievements, a second look at our results reveals that the design and optimization of soft ROCK inhibitors (and, likely, soft kinase inhibitors in general) cannot be summarized into the mere addition of an ester function to an existing scaffold. To start with, it is likely that the difference of functional activity observed in the MLC-PP assay results at least in part from a difference of cell permeability

between the parent compound and its carboxylic acid metabolite. Playing upon differences in physicochemical properties to modulate compound efficacy is a well-known strategy in medicinal chemistry, which has been used extensively – but in the opposite direction – for the design of prodrugs. This strategy appears well suited to the current compound series, which displayed from the start acceptable -but not excellent- permeability. However, it can also be seen as a double-edged sword, as we observed that even introduction of a moderately polar functional group on the parent compound could result in weaker EC_{50} values in the MLC-PP assay. Optimization of soft ROCK inhibitors relying on differences of permeability should therefore be done carefully. Another interesting observation is the diversity of profiles resulting from the addition of ester groups to parent molecules. Large differences in hydrolysis rates were indeed observed between compounds, depending not only on the nature of the ester group, but also on its position. This situation is easily understandable, as hydrolysis of the ester group does not result from chemical instability, but rather from metabolism by esterases, as demonstrated by esterase inhibition experiments. Consequently, recognition as an esterase substrate is a fundamental step in the inactivation of the soft drug. It is likely that some ester functions allowing a high inactivation rate when put on one position on one scaffold are still unable to provide a sufficient rate when placed on another position or scaffold. The striking difference of stability of compound **8** in plasma or in presence of hepatocytes also poses the question of stability in different target organs. Esterases are indeed expressed in different levels, depending on organ, or even tissue. For instance, differences in the expression of carboxylesterase 1, which preferentially hydrolyzes esters from small alcohol groups and carboxylesterase 2, which favors hydrolysis of esters from bulkier alcohol groups,[36] are found between liver, lung or intestine.[37] Such differences in plasma and organ stability might ultimately influence the potential

indications of a soft ROCK inhibitor. For instance, compounds with relatively fast degradation rate in plasma, such as **13** or **18**, appear more adapted for indications where there is a significant risk of high systemic exposure following administration. Oral administration for treatment of intestinal diseases and administration through inhalation for treatment of lung diseases represent potential examples of such applications. At the other side of the spectrum, compound **8** appears quite stable in plasma, and might essentially be degraded in liver, as indicated by hepatocyte and PK data. This compound could however be of particular interest for sustained release strategies, where the limited amount of drug that can be encapsulated into a matrix imposes the use of a very potent compound. The soft drug approach implemented within this compound could then be used to minimize the effects of an initial burst release occurring after administration, which could otherwise still lead to an unacceptable systemic concentration.

Conclusion

We have here presented the design, synthesis and evaluation of a novel series of soft ROCK inhibitors; more precisely benzoic or phenacetic ester analogues of 4-(aminomethyl)-N-(pyridin-4-yl)-3[3-(phenylcarbamoyl) phenyl] benzamide (**2**). The resulting compounds display low nanomolar or sub-nanomolar on-target activity, as well as functional activity in cell-based assays including MLC phosphorylation and wound healing assay. Upon entering systemic circulation, these inhibitors should be rapidly inactivated by blood or liver esterases, thereby reducing the risk of systemic ROCK-associated side effects. The stability profile of those compounds can be modulated by altering the nature and position of the ester moiety they contain, suggesting that they might cover a range of potential indications for which local administration is applicable. Further *in vivo* evaluation of compounds resulting from this work will be presented in due time.

Experimental section

Molecular modeling

2D compound structures were drawn in Instant *JChem v6.3.3*. The protonation state of the molecules was adjusted based on predicted pKa values, and the resulting structures were exported as SMILES strings. Initial 3D structures were generated with *openbabel*, using the *obgen* and *obminimize* tools and the mmff94 forcefield. 3D structures were manually inspected before further modeling. Ligand files for molecular docking were then produced with *AutodockTools 1.5.4.*

The receptor model used for docking was initially based on the ROCK2 crystal structure 2ETR. Receptor files were later updated once the crystal structure of compound **10** with ROCK2 had been obtained. Whenever necessary, missing residues or loops were rebuilt with *Yasara Structure*, using the YASARA2 forcefield and the available homology modeling, model refinement and template forcing routines. The docking grids were generated with *AutodockTools 1.5.4 and Autogrid4.* Default parameters were used, except for grid step size, which was reduced from 0.33 A to 0.25 A in order to obtain a more accurate docking grid.

Molecular docking was carried out using *Autodock 4.2.* Default parameters were mostly used. However, we observed that docking quality was increased by adapting some of the parameters based on the number of rotatable bonds (nrot) in the ligand with the following changes. The genetic algorithm population size was 150 (default) for nrot <9 or 150 + (25 x (nrot - 8)) for nrot ≥9. The maximal number of energy evaluations per run was 1000000 + (nrot x 250000) for nrot

<9 or 3000000+(1000000 x (nrot-8)) for nrot ≥9. The number of genetic algorithm runs was increased from 10 to 30 in all cases.

Docking poses were refined with *Yasara*, using the YASARA2 forcefield. The ROCK2-inhibitor complex structure was modeled in a periodic water box, which was kept neutral by addition of Na^+ or Cl^- ions. Final simulated NaCl concentration was 0.9%. Steepest descent and simulating annealing routines implemented within *Yasara* were used as such for energy minimization.

All docking and crystal structure pictures were generated with *Pymol.*

Chemistry:

General Methods:

All reagents and solvents were of commercial quality and were used without further purification. The purity of the final compounds and/or intermediates was characterized by high-performance liquid chromatography (HPLC) using a Waters Alliance system with a 2690 separation module, coupled to a 996 Waters photodiode array detector (PDA) and ZMD Micromass MS system simultaneously. The analytical column was a reversed-phase TSKgel Super-ODS C18 2 μm, 50 mm x 4.6 mm, from Tosoh Bioscience, used at a column temperature of 55 °C. A gradient elution was used (flow 2.75 mL/min), typically starting with 100% water and progressing to 100% acetonitrile over a period of 5 min, with both solvents containing 0.1% formic acid. All compounds have >95% purity as determined by HPLC (diode array detector, 200-400 nm). All masses were reported as those of the protonated parent ions (molecular weight range 100−800, cone voltage 25 V). ^1H and ^{13}C NMR spectra were taken on a Varian Inova 300 or 400 MHz spectrometer from solutions in deuterated DMSO. The chemical shifts were calibrated by means

of the residual proton and carbon resonance signals of DMSO-*d6* (2.50 and 39.52 ppm for ^{1}H and ^{13}C, respectively).

General procedure 1: Suzuki coupling

To a solution of compound **3** (36.50 g, 0.086 mol, 1.0 eq) and 3-carboxyphenylboronic acid (14.27 g, 0.086 mol, 1.0 eq) or 3-aminophenylboronic acid (11.78 g, 0.086 mol, 1.0 eq) in DMF (350 mL) and H_2O (87.5 mL) was added Na_2CO_3 (18.23 g, 0.172 mol, 2.0 eq). Then $Pd(dppf)Cl_2$ (3.15 g, 0.0043 mol, 0.05 eq) was added to the solution under inert atmosphere (N_2) and the resulting solution was stirred at 100 °C for 16h. The solvent was evaporated under vacuum and the residue was purified by column chromatography on silica gel using DCM/MeOH 10:1 to yield the desired biphenyl derivative **4** or **5**.

General procedure 2: Amide bond formation

Protocol A. To a suspension of intermediate **4** (1.0 g, 2.148 mmol, 1.0 eq) and an appropriate aniline derivative (2.158 mmol, 1.2 eq) in DCM (15 mL) at 0 °C were added T3P (3.84 mL, 50% w/w in EtOAc, 6.45 mmol, 3.0 eq) dropwise and DMAP (1.050 g, 8.59 mmol, 4.0 eq). The resulting solution was stirred at room temperature for 2 hours and diluted with EtOAc. The organic layer was washed with saturated sodium bicarbonate, ammonium chloride, bicarbonate, and brine solution subsequently, dried over sodium sulfate, filtered and concentrated. The residue was purified by column chromatography on silica gel using DCM/MeOH to yield the desired products.

Protocol B. To a suspension of intermediate **5** (1.0 g, 2.291 mmol, 1.0 eq) and an appropriate benzoic acid derivative (2.405 mmol, 1.05 eq) in DCM (15 mL) at 0 °C were added T3P (4.36 mL, 50% w/w in EtOAc, 7.331 mmol, 3.2 eq) dropwise and DMAP (1.050 g, 9.622 mmol, 4.2

eq). The resulting solution was stirred at room temperature for 2 hours and diluted with EtOAc. The organic layer was washed with saturated sodium bicarbonate, ammonium chloride, sodium bicarbonate, and brine solution subsequently, dried over sodium sulfate, filtered and concentrated. The residue was purified by column chromatography on silica gel using DCM/MeOH to yield the desired products.

General procedure 3: Methyl ester hydrolysis

To a solution of the methyl ester (2.0 mmol, 1.0 eq) intermediate in THF (6 mL) was added a solution of lithium hydroxide (144 mg, 6.0 mmol, 3.0 eq) in water (3 mL) and the resulting solution was stirred at room temperature for 2 hours. When complete conversion was achieved, the organic solvent was evaporated under reduced pressure, and the pH of the aqueous solution was adjusted to pH=6 by addition of an aqueous 1M HCl solution, resulting in precipitation. The white precipitate was collected by filtration, washed with water (3x) and dried to yield the desired carboxylic acid derivative.

General procedure 4: Esterification

To a suspension of carboxylic acid intermediate (150 mg, 1.0 eq), an appropriate alcohol (3.0 eq) and DMAP (4.0 eq) in DCM (2 mL) at 0 °C was added T3P (50% w/w in EtOAc, 3.0 eq) dropwise. The resulting solution was stirred at room temperature for 2 hours and diluted with EtOAc. The organic layer was washed with saturated sodium bicarbonate, ammonium chloride, sodium bicarbonate, and brine solution subsequently, dried over sodium sulfate, filtered and concentrated. The residue was purified by column chromatography on silica gel using DCM/MeOH to yield the desired products.

General procedure 5: Boc-deprotection

Protocol A. The ester (or carboxylic acid) intermediate was dissolved in DCM/TFA (7:1) and the reaction mixture was stirred at room temperature for 16 hours or until LC-MS analysis showed complete conversion. Then the reaction mixture was concentrated and the crude product was purified by reversed phase column chromatography to give the final products.

Protocol B. The ester (or carboxylic acid) intermediate was dissolved in DCM and HCl gas was bubbled for 5-15 minutes and then the reaction mixture was stirred at room temperature for 1-16 h. When LC-MS showed the reaction was complete, the reaction mixture was concentrated and the crude product was purified by preparative HPLC to give the final products.

The compounds below were synthesized using the general procedures above (see Scheme 1 for the reaction sequence).

Methyl 4-{[(2'-(aminomethyl)-5'-{[(3-fluoropyridin-4-yl)amino]carbonyl}biphenyl-3-yl)carbonyl]amino}benzoate, HCl salt (2)

^{1}H NMR (DMSO-*d6*, 300 MHz): δ 11.21 (s, 1H), 10.52 (s, 1H), 8.91 (d, 1H, *J* = 3.7 Hz), 8.76-8.63 (m, 3H), 8.57 (d, 1H, *J* = 5.9 Hz), 8.29 (t, 1H, *J* = 6.3 Hz), 8.21 (br s, 1H), 8.14-8.05 (m, 3H), 7.94 (d, 1H, *J* = 8.0 Hz), 7.86 (d, 2H, *J* = 7.7 Hz), 7.75-7.64 (m, 2H), 7.34 (t, 2H, *J* = 7.8 Hz), 7.10 (t, 1H, *J* = 7.3 Hz), 4.12-4.01 (m, 2H). MS, *m/z*: 441.01 $(M + H)^+$.

2'-{[(*Tert*-butoxycarbonyl)amino]methyl}-5'-{[(3-fluoropyridin-4-yl)amino]carbonyl}biphenyl-3-carboxylic acid (4)

^{1}H NMR (DMSO-*d6*, 300 MHz): δ 13.11 (br s, 1H), 10.53 (s, 1H), 8.59 (d, 1H, *J* = 2.6 Hz), 8.39 (d, 1H, *J* = 5.3 Hz), 8.12-7.80 (m, 5H), 7.78-7.37 (m, 4H), 4.12 (d, 2H, *J* = 5.8 Hz), 1.37 (s, 9H).

^{13}C NMR (DMSO-*d6*, 100 MHz): δ 167.3, 165.6, 155.8, 151.3, 146.3, 141.8, 139.9, 139.5, 138.2, 133.7, 133.6, 132.0, 131.2, 129.9, 129.4, 128.8, 128.6, 127.8, 127.5, 118.7, 78.2, 41.5, 28.3. MS, *m/z*: 466.05 $(M + H)^+$.

Tert-butyl [(3'-amino-5-{[(3-fluoropyridin-4-yl)amino]carbonyl}biphenyl-2-yl)methyl]carbamate (5)

^{1}H NMR (DMSO-*d6*, 300 MHz): δ 10.47 (s, 1H), 8.59 (d, 1H, *J* = 2.6 Hz), 8.39 (d, 1H, *J* = 5.3 Hz), 8.04-7.85 (m, 2H), 7.85-7.75 (m, 1H), 7.70-7.32 (m, 2H), 7.11 (t, 1H, *J* = 7.7 Hz), 6.70-6.42 (m, 3H), 5.20 (s, 2H), 4.16 (d, 2H, *J* = 5.8 Hz), 1.40 (s, 9H). ^{13}C NMR (DMSO-*d6*, 100 MHz): δ 165.6, 155.9, 151.3, 148.7, 146.2, 141.7, 141.2, 140.1, 138.1, 133.5, 131.5, 129.0, 128.9, 126.9, 126.6, 118.6, 116.6, 114.6, 113.1, 78.0, 41.5, 28.2. MS, *m/z*: 437.33 $(M + H)^+$.

Methyl 3-{[(2'-(aminomethyl)-5'-{[(3-fluoropyridin-4-yl)amino]carbonyl}biphenyl-3-yl)carbonyl]amino}benzoate, TFA salt (6)

^{1}H NMR (DMSO-*d6*, 300 MHz): δ 10.68 (s, 1H), 10.57 (s, 1H), 8.83 (d, 1H, *J* = 2.6 Hz), 8.47 (t, 1H, *J* = 1.8 Hz), 8.42 (d, 1H, *J* = 5.3 Hz), 8.42-8.22 (m, 3H), 8.17-8.06 (m, 4H), 8.04 (d, 1H, *J* = 1.8 Hz), 7.93 (dd, 1H, *J* = 5.5, 6.6 Hz), 7.82 (d, 1H, *J* = 8.2 Hz), 7.78-7.66 (m, 3H), 7.53 (t, 1H, *J* = 8.0 Hz), 4.10 (q, 2H, *J* = 5.6 Hz), 3.87 (s, 3H). MS, *m/z*: 499.14 $(M + H)^+$.

Methyl (3-{[(2'-(Aminomethyl)-5'-{[(3-fluoropyridin-4-yl)amino]carbonyl}biphenyl-3-yl)carbonyl]amino}phenyl)acetate, TFA salt (7)

^{1}H NMR (DMSO-*d6*, 400 MHz): δ 10.67 (s, 1H), 10.36 (s, 1H), 8.63 (d, 1H, J = 2.5 Hz), 8.42 (d, 1H, J = 5.3 Hz), 8.30 (br s, 3H), 8.13 (dd, 1H, J = 8.1, 1.5 Hz), 8.10-8.02 (m, 3H), 7.92 (t, 1H, J

= 6.0 Hz), 7.81 (d, 1H, J = 8.2 Hz), 7.69 (br s, 4H), 7.31 (t, 1H, J = 8.2 Hz), 7.02 (d, 1H, J = 7.5 Hz), 4.09 (q, 2H, J = 5.6 Hz), 3.68 (s, 2H), 3.62 (s, 3H). MS, *m/z*: 513.24 $(M + H)^+$.

Methyl 4-{[(2'-(aminomethyl)-5'-{[(3-fluoropyridin-4-yl)amino]carbonyl}biphenyl-3-yl)carbonyl]amino}benzoate, HCl salt (8)

^{1}H-NMR (DMSO-*d6*, 300 MHz): δ 11.18 (s, 1H), 10.88 (s, 1H), 8.91 (d, 1H, *J* = 3.7 Hz), 8.81-8.63 (m, 3H), 8.57 (d, 1H, *J* = 5.9 Hz), 8.36-8.19 (m, 2H), 8.18-8.01 (m, 5H), 8.01-7.88 (m, 3H), 7.80-7.64 (m, 2H), 4.20-3.96 (m, 2H), 3.83 (s, 3H). MS, *m/z*: 499.04 $(M + H)^+$.

Methyl (4-{[(2'-(aminomethyl)-5'-{[(3-fluoropyridin-4-yl)amino]carbonyl}biphenyl-3-yl)carbonyl]amino}phenyl)acetate, HCl salt (9)

^{1}H NMR (DMSO-*d6*, 400 MHz): δ 11.05 (s,1H), 10.51 (s, 1H), 8.81 (d, 1H, *J* = 3.3 Hz), 8.65 (br s, 3H), 8.52 (d, 1H, *J* = 5.7 Hz), 8.21 (s, 1H), 8.15 (t, 1H, *J* = 6.2 Hz), 8.11 (dd, 1H, *J* = 8.2, 1.4 Hz), 8.09-8.03 (m, 2H), 7.93 (d, 1H, *J* = 8.1 Hz), 7.79 (d, 2H, *J* = 8.5 Hz), 7.74-7.64 (m, 2H), 7.24 (d, 2H, *J* = 8.4 Hz), 4.14-3.99 (m, 2H), 3.65 (s, 2H), 3.61 (s, 3H). MS, *m/z*: 513.08 $(M + H)^+$.

Isopropyl 3-{[(2'-(aminomethyl)-5'-{[(3-fluoropyridin-4-yl)amino]carbonyl}biphenyl-3-yl)carbonyl]amino}benzoate, HCl salt (10)

^{1}H NMR (DMSO-*d6*, 400 MHz): δ 11.07 (s, 1H), 10.71 (s, 1H), 8.83 (d, 1H, *J* = 3.5 Hz), 8.80-8.55 (m, 3H), 8.53 (d, 1H, *J* = 5.8 Hz), 8.48 (t, 1H, *J* = 1.8 Hz), 8.26-8.08 (m, 5H), 8.08 (d, 1H, *J* = 1.8 Hz), 7.94 (d, 1H, *J* = 8.2 Hz), 7.78-7.64 (m, 3H), 7.50 (t, 1H, *J* = 8.0 Hz), 5.15 (sept, 1H, *J* = 6.2 Hz), 4.07 (q, 2H, *J* = 5.6 Hz), 1.32 (d, 6H, J = 6.2 Hz). MS, *m/z*: 527.09 $(M + H)^+$.

Butyl 3-{[(2'-(aminomethyl)-5'-{[(3-fluoropyridin-4-yl)amino]carbonyl}biphenyl-3-yl)carbonyl]amino}benzoate, HCl salt (11)

^{1}H NMR (DMSO-*d6*, 400 MHz): δ 11.09 (s, 1H), 10.73 (s, 1H), 8.85 (d, 1H, *J* = 3.5 Hz), 8.78-8.58 (m, 3H), 8.54 (d, 1H, *J* = 5.8 Hz), 8.51 (t, 1H, *J* = 1.8 Hz), 8.26-8.07 (m, 5H), 8.08 (d, 1H, *J* = 1.8 Hz), 7.94 (d, 1H, *J* = 8.2 Hz), 7.78-7.65 (m, 3H), 7.51 (t, 1H, *J* = 8.0 Hz), 4.29 (t, 2H, *J* = 6.5 Hz), 4.07 (q, 2H, *J* = 5.6 Hz), 1.75-1.63 (m, 2H), 1.50-1.36 (m, 2H), 0.93 (t, 3H, *J* = 7.4 Hz). MS, *m/z*: 541.10 $(M + H)^+$.

***Sec-butyl* 3-{[(2'-(aminomethyl)-5'-{[(3-fluoropyridin-4-yl)amino]carbonyl}biphenyl-3-yl)carbonyl]amino}benzoate, TFA salt (12)**

^{1}H NMR (DMSO-*d6*, 300 MHz): δ 10.67 (s, 1H), 10.57 (s, 1H), 8.63 (d, 1H, *J* = 2.7 Hz), 8.52-8.38 (m, 2H), 8.38-8.22 (m, 3H), 8.17-8.05 (m, 4H), 8.03 (d, 1H, *J* = 1.7 Hz), 7.93 (dd, 1H, *J* = 5.6, 6.6 Hz), 7.81 (d, 1H, *J* = 8.2 Hz), 7.76-7.67 (m, 3H), 7.52 (t, 1H, *J* = 8.0 Hz), 8.07-4.94 (m, 1H), 4.16-4.04 (m, 2H), 1.74-1.62 (m, 2H), 1.29 (d, 2H, *J* = 6.3 Hz), 1.00-0.86 (t, 3H, *J* = 7.4 Hz). MS, *m/z*: 541.13 $(M + H)^+$.

Methyl 3-{[(2'-(aminomethyl)-5'-{[(3-fluoropyridin-4-yl)amino]carbonyl}biphenyl-3-yl)carbonyl]amino}-4-fluorobenzoate, HCl salt (13)

^{1}H NMR (DMSO-*d6*, 400 MHz): δ 11.16 (s, 1H), 10.63 (s, 1H), 8.90 (d, 1H, *J* = 3.8 Hz), 8.82-8.60 (m, 3H), 5.56 (d, 1H, *J* = 5.9 Hz), 8.31-8.23 (m, 2H), 8.23-8.18 (m, 1H), 8.15-8.07 (m, 2H), 8.07-8.04 (d, 1H, *J* = 1.9 Hz), 7.95 (d, 1H, *J* = 8.2 Hz), 7.88 (ddd, 1H, *J* = 8.6, 4.7, 2.3 Hz), 7.76 (dt, 1H, *J* = 7.7, 1.4 Hz), 7.70 (t, 1H, *J* = 7.6 Hz), 7.47 (dd, 1H, *J* = 10.1, 7.7 Hz), 4.08 (q, 2H, *J* = 5.6 Hz), 3.86 (s, 3H). MS, *m/z*: 517.11 $(M + H)^+$.

Propyl 3-{[(2'-(aminomethyl)-5'-{[(3-fluoropyridin-4-yl)amino]carbonyl}biphenyl-3-yl)carbonyl]amino}-4-fluorobenzoate, HCl salt (14)

^{1}H NMR (DMSO-*d6*, 400 MHz): δ 10.80 (s, 1H), 10.57 (s, 1H), 8.67 (s, 1H), 8.58 (br s, 3H), 8.44 (d, 1H, *J* = 3.6 Hz), 8.25 (d, 1H, *J* = 6.0 Hz), 8.17 (s, 1H), 8.14-8.09 (m, 2H), 8.05 (s, 1H), 8.01-7.94 (m, 1H), 7.94-7.84 (m, 2H), 7.79-7.64 (m, 2H), 7.47 (t, 1H, *J* = 9.2 Hz), 4.24 (t, 2H, *J* = 6.2 Hz), 4.08 (d, 2H, *J* = 4.2 Hz), 1.72 (q, 2H, *J* = 6.9 Hz), 0.97 (t, 3H, *J* = 7.2 Hz). MS, *m/z*: 545.18 $(M + H)^+$.

(1*S*)-1-Methylpropyl 3-{[(2'-(aminomethyl)-5'-{[(3-fluoropyridin-4-yl)amino]carbonyl}biphenyl-3-yl)carbonyl]amino}-4-fluorobenzoate, HCl salt (15)

^{1}H NMR (DMSO-*d6*, 300 MHz): δ 11.03 (s, 1H), 10.60 (s, 1H), 8.81 (d, 1H, *J* = 3.4 Hz), 8.76-8.57 (m, 3H), 8.52 (d, 1H, *J* = 5.7 Hz), 8.30-8.02 (m, 6H), 7.97-7.83 (m, 2H), 8.79-8.65 (m, 2H), 7.46 (dd, 2H, *J* = 10.1, 8.8 Hz), 4.99 (sext, 1H, *J* = 6.2 Hz), 4.16-3.98 (m, 2H), 1.77-1.58 (m, 2H), 1.28 (d, 3H, *J* = 6.3 Hz), 0.91 (t, 3H, *J* = 7.4 Hz). MS, *m/z*: 559.17 $(M + H)^+$.

(1*R*)-1-Methylpropyl 3-{[(2'-(aminomethyl)-5'-{[(3-fluoropyridin-4-yl)amino]carbonyl}biphenyl-3-yl)carbonyl]amino}-4-fluorobenzoate, HCl salt (16)

^{1}H NMR (DMSO-*d6*, 300 MHz): δ 11.06 (s, 1H), 10.61 (s, 1H), 8.82 (d, 1H, *J* = 3.5 Hz), 8.66 (br s, 3H), 8.52 (d, 1H, *J* = 5.8 Hz), 8.28-8.07 (m, 5H), 8.05 (d, 1H, *J* = 1.7 Hz), 7.93 (d, 1H, *J* = 8.2 Hz), 7.88 (ddd, 1H, *J* = 8.6, 4.7, 2.3 Hz), 7.79-7.66 (m, 2H), 7.46 (dd, 2H, *J* = 10.1, 8.8, Hz), 4.99 (sext, 1H, *J* = 6.2 Hz), 4.08 (q, 2H, *J* = 5.5 Hz), 1.77-1.56 (m, 2H), 1.28 (d, 3H, *J* = 6.2), 0.91 (t, 3H, *J* = 7.4). MS, *m/z*: 559.19 $(M + H)^+$.

Methyl 3-{[(2'-(aminomethyl)-5'-{[(3-fluoropyridin-4-yl)amino]carbonyl}biphenyl-3-yl)amino]carbonyl}benzoate, HCl salt (17)

^{1}H NMR (DMSO-*d6*, 400 MHz): δ 11.04 (s, 1H), 10.74 (s, 1H), 8.86 (d, 1H, *J* = 3.4 Hz), 8.69 (br s, 3H), 8.58-8.56 (s, 1H), 8.54 (d, 1H, *J* = 5.8 Hz), 8.31 (d, 1H, *J* = 7.9 Hz), 8.22 (t, 1H, *J* = 6.3 Hz), 8.17 (d, 1H, *J* = 7.8 Hz), 8.11 (dd, 1H, *J* = 8.1, 1.6 Hz), 8.01-7.85 (m, 4H), 7.71 (t, 1H, *J* = 7.8 Hz), 7.53 (t, 1H, *J* = 7.9 Hz), 7.27 (d, 1H, *J* = 7.6 Hz), 4.14-4.04 (m, 2H), 3.91 (s, 3H). MS, *m/z*: 499.14 $(M + H)^+$.

Propyl 3-{[(2'-(aminomethyl)-5'-{[(3-fluoropyridin-4-yl)amino]carbonyl}biphenyl-3-yl)amino]carbonyl}benzoate, HCl salt (18)

^{1}H NMR (DMSO-*d6*, 400 MHz): δ 10.96 (s, 1H), 10.74 (s, 1H), 8.80 (d, 1H, *J* = 3.3 Hz), 8.68 (br s, 3H), 8.55 (t, 1H, *J* = 1.6 Hz), 8.51 (d, 1H, *J* = 5.7 Hz), 8.31 (dt, 1H, *J* = 7.8, 1.1 Hz), 8.19-8.13 (m, 2H), 8.11 (dd, 1H, *J* = 8.2, 1.8 Hz), 7.98 (d, 1H, *J* = 1.8 Hz), 7.95 (t, 1H, *J* = 1.7 Hz), 7.92 (d, 1H, *J* = 8.2 HZ), 7.89 (d, 1H, *J* = 8.2 Hz), 7.71 (t, 1H, *J* = 7.8 Hz), 7.53 (t, 1H, *J* = 7.9 Hz), 7.26 (d, 1H, *J* = 7.8 Hz), 4.28 (t, 2H, *J* = 6.6 Hz), 4.13-4.05 (m, 2H), 1.75 (sextet, 2H, *J* = 7.1 Hz), 0.98 (t, 3H, *J* = 7.4 Hz). MS, *m/z*: 527.16 $(M + H)^+$.

Methyl 3-{[(2'-(aminomethyl)-5'-{[(3-fluoropyridin-4-yl)amino]carbonyl}biphenyl-3-yl)amino]carbonyl}-4-fluorobenzoate, TFA salt (19)

Due to limited commercial availability of 2-fluoro-5-(methoxycarbonyl)benzoic acid, compound **19** was not synthesized using the general scheme and methods. For the synthetic route and protocols, we refer to the Supporting Information.

^{1}H NMR (DMSO-*d6*, 300 MHz): δ 10.76 (s, 1H), 10.65 (s, 1H), 8.63 (d, 1H, *J* = 2.8 Hz), 8.42 (d, 1H, *J* = 5.3 Hz), 8.36-8.22 (m, 3H), 8.24 (dd, 1H, *J* = 6.7, 2.3 Hz), 8.21-8.13 (m, 1H), 8.11 (dd, 1H, *J* = 8.1, 1.8 Hz), 7.99 (d, 1H, *J* = 3.8 Hz), 7.92 (dd, 1H, *J* = 6.6, 5.5 Hz), 7.90-7.85 (m, 1H), 7.79 (d, 1H, *J* = 8.2 Hz), 7.76-7.69 (m, 1H), 7.60-7.49 (m, 2H), 7.28-7.21 (m, 1H), 4.18-4.06 (m, 2H), 3.89 (s, 3H). MS, *m/z*: 517.07 $(M + H)^+$.

2-Methoxyethyl 3-{[(2'-(aminomethyl)-5'-{[(3-fluoropyridin-4-yl)amino]carbonyl}biphenyl-3-yl)amino]carbonyl}-4-fluorobenzoate, HCl salt (20)

Due to limited commercial availability of 2-fluoro-5-(methoxycarbonyl)benzoic acid, compound **20** was not synthesized using the general scheme and methods. For the synthetic route and protocols, we refer to the Supporting Information.

^{1}H NMR (DMSO-*d6*, 400 MHz): δ 10.90 (s, 1H), 10.82 (s, 1H), 8.77 (s, 1H), 8.63 (br s, 3H), 8.49 (d, 1H, *J* = 5.3 Hz), 8.23 (d, 1H, *J* = 5.3 Hz), 8.19-8.06 (m, 3H), 7.97 (s, 1H), 7.91 (d, 1H, *J* = 8.1 Hz), 7.87 (s, 1H), 7.76 (d, 1H, *J* = 7.6 Hz), 7.60-7.46 (m, 2H), 7.27 (d, 1H, *J* = 7.0 Hz), 4.43 (br s, 2H), 4.13-3.97 (m, 2H), 3.67 (br s, 2H), 3.30 (s, 3H). MS, *m/z*: 561.18 $(M + H)^+$.

Methyl 3-{[(2'-(aminomethyl)-5'-{[(3-fluoropyridin-4-yl)amino]carbonyl}biphenyl-3-yl)carbonyl]amino}-2-fluorobenzoate, HCl salt (21)

^{1}H NMR (DMSO-*d6*, 400 MHz): δ 10.95 (s, 1H), 10.52 (s, 1H), 8.78 (d, 1H, J = 3.2 Hz), 8.57 (br s, 3H), 8.50 (d, 1H, J = 5.6 Hz), 8.17 (br s, 1H), 8.14-8.08 (m, 3H), 8.05 (d, 1H, J = 1.8 Hz), 7.90 (d, 1H, J = 8.2 Hz), 7.86 (td, 1H, J = 7.5, 1.6 Hz), 7.78-7.68 (m, 3H), 7.34 (t, 1H, J = 7.9 Hz), 4.09 (q, 2H, J = 5.6 Hz), 3.87 (s, 3H). MS, *m/z*: 517.20 $(M + H)^+$.

Cyclopentyl 3-{[(2'-(aminomethyl)-5'-{[(3-fluoropyridin-4-yl)amino]carbonyl}biphenyl-3-yl)carbonyl]amino}-2-fluorobenzoate, HCl salt (22)

^{1}H NMR (DMSO-*d6*, 400 MHz): δ 10.88 (s, 1H), 10.48 (s, 1H), 8.74 (s, 1H), 8.58-8.45 (m, 4H), 8.17-8.01 (m, 5H), 7.92-7.81 (m, 2H), 7.77-7.67 (m, 3H), 7.34 (t, 1H, J = 7.9 Hz), 5.35 (s, 1H), 4.08 d, 2H, J = 5.1 Hz), 1.98-1.86 (m, 2H), 1.80-1.55 (m, 6H). MS, *m/z*: 571.27 $(M + H)^+$.

Isopropyl (4-{[(2'-(aminomethyl)-5'-{[(3-fluoropyridin-4-yl)amino]carbonyl}biphenyl-3-yl)carbonyl]amino}phenyl)acetate, HCl salt (23)

^{1}H NMR (DMSO-*d6*, 400 MHz): δ 11.13 (s, 1H), 10.51 (s, 1H), 8.87 (d, 1H, *J* = 3.6 Hz), 8.66 (br s, 3H), 8.55 (d, 1H, *J* = 3.6 Hz), 8.26 - 8.18 (m, 2H), 8.11 (dd, 1H, *J* = 8.2, 1.9 Hz), 8.09-8.05 (m, 2H), 7.93 (d, 1H, *J* = 8.2 Hz), 7.79 (d, 2H, *J* = 8.6 Hz), 7.73-7.65 (m, 2H), 7.23 (d, 2H, *J* = 8.6 Hz), 4.89 (sept, 1H, *J* = 6.2 Hz), 4.06 (q, 2H, *J* = 5.6 Hz), 3.59 (s, 2H), 1.18 (d, 6H, *J* = 6.2 Hz). MS, *m/z*: 541.17 $(M + H)^+$.

(1*S*)-1-Methylpropyl (4-{[(2'-(aminomethyl)-5'-{[(3-fluoropyridin-4-yl)amino]carbonyl}biphenyl-3-yl)carbonyl]amino}phenyl)acetate, HCl salt (24)

^{1}H NMR (DMSO-*d6*, 400 MHz): δ 11.08 (s, 1H), 10.50 (s, 1H), 8.84 (d, 1H, *J* = 3.2 Hz), 8.64 (br s, 3H), 8.53 (d, 1H, *J* = 5.7 Hz), 8.23-8.15 (m, 2H), 8.14-8.03 (m, 3H), 7.92 (d, 1H, *J* = 8.2 Hz), 7.79 (d, 2H, *J* = 8.4 Hz), 7.73-7.65 (m, 2H), 7.24 (d, 2H, *J* = 8.4 Hz), 4.74 (sext, 1H, *J* = 6.2 Hz), 4.07 (q, 2H, *J* = 5.4 Hz), 3.60 (s, 2H), 1.51 (m, 2H), 1.15 (d, 3H, *J* = 6.2 Hz), 0.80 (t, 3H, *J* = 7.4 Hz). MS, *m/z*: 555.23 $(M + H)^+$.

(1*R*)-1-Methylpropyl (4-{[(2'-(aminomethyl)-5'-{[(3-fluoropyridin-4-yl)amino]carbonyl}biphenyl-3-yl)carbonyl]amino}phenyl)acetate, HCl salt (25)

^{1}H NMR (DMSO-*d6*, 400 MHz): δ 11.06 (s, 1H), 10.50 (s, 1H), 8.82 (d, 1H, *J* = 3.4 Hz), 8.64 (br s, 3H), 8.52 (d, 1H, *J* = 5.7 Hz), 8.21-8.14 (m, 2H), 8.11 (dd, 1H, *J* = 8.1, 1.7 Hz), 8.09-8.04 (m, 2H), 7.92 (d, 1H, *J* = 8.2 Hz), 7.79 (d, 2H, *J* = 8.5 Hz), 7.73-7.65 (m, 2H), 7.24 (d, 2H, *J* = 8.5 Hz), 4.74 (sext, 1H, *J* = 6.3 Hz), 4.07 (q, 2H, *J* = 5.5 Hz), 3.60 (s, 2H), 1.56-1.45 (m, 2H), 1.14 (d, 3H, *J* = 6.3 Hz), 0.80 (t, 3H, *J* = 7.4 Hz). MS, *m/z*: 555.24 $(M + H)^+$.

Tetrahydro-2*H*-pyran-4-yl (4-{[(2'-(aminomethyl)-5'-{[(3-fluoropyridin-4-yl)amino]carbonyl}biphenyl-3-yl)carbonyl]amino}phenyl)acetate, TFA salt (26)

^{1}H NMR (DMSO-*d6*, 400 MHz): δ 10.71 (s, 1H), 10.35 (s, 1H), 8.65 (d, 1H, *J* = 2.8 Hz), 8.43 (d, 1H, *J* = 5.4 Hz), 8.32 (br s, 3H), 8.12 (dd, 1H, *J* = 8.2, 1.9 Hz), 8.09-8.05 (m, 1H), 8.05-8.01 (m, 2H), 7.95 (dd, 1H, *J* = 6.6, 5.5 Hz), 7.81 (d, 1H, *J* = 8.2 Hz), 7.73 (d, 2H, *J* = 8.6 Hz), 7.71-7.68 (m, 2H), 7.26 (d, 2H, *J* = 8.6 Hz), 4.87 (septet, 1H, *J* = 4.3 Hz), 4.15-4.05 (m, 2H), 3.79-3.70 (m, 2H), 3.65 (s, 2H), 3.43 (ddd, 2H, *J* = 11.7, 9.0, 2.9 Hz), 1.88-1.77 (m, 2H), 1.58-1.46 (m, 2H). MS, *m/z*: 583.01 $(M + H)^+$.

Cyclobutyl (4-{[(2'-(aminomethyl)-5'-{[(3-fluoropyridin-4-yl)amino]carbonyl}biphenyl-3-yl)carbonyl]amino}phenyl)acetate, HCl salt (27)

^{1}H NMR (DMSO-*d6*, 400 MHz): δ 11.10 (s, 1H), 10.51 (s, 1H), 8.85 (d, 1H, *J* = 3.6 Hz), 8.65 (br s, 3H), 8.54 (d, 1H, *J* = 5.8 Hz), 8.25-8.16 (m, 2H), 8.11 (dd, 1H, *J* = 8.1, 1.9 Hz), 8.09-8.04 (m, 2H), 7.92 (d, 1H, *J* = 8.2 Hz), 7.79 (d, 2H, *J* = 8.6 Hz), 7.74-7.64 (m, 2H), 7.23 (d, 2H, *J* = 8.6 Hz), 4.96-4.84 (m, 1H), 4.13-4.02 (m, 2H), 3.61 (s, 2H), 2.31-2.19 (m, 2H), 2.05-1.92 (m, 2H), 1.78-1.66 (m, 1H), 1.65-1.50 (m, 1H). MS, *m/z*: 553.14 $(M + H)^+$.

Cyclopentyl (4-{[(2'-(aminomethyl)-5'-{[(3-fluoropyridin-4-yl)amino]carbonyl}biphenyl-3-yl)carbonyl]amino}phenyl)acetate, HCl salt (28)

^{1}H NMR (DMSO-*d6*, 400 MHz): δ 11.05 (s, 1H), 10.50 (s, 1H), 8.81 (d, 1H, *J* = 3.4 Hz), 8.65 (br s, 3H), 8.52 (d, 1H, *J* = 5.7 Hz), 8.19 (br s, 1H), 8.15 (t, 1H, *J* = 6.3 Hz), 8.11 (dd, 1H, *J* = 8.1, 1.9 Hz), 8.09-8.03 (m, 2H), 7.92 (d, 1H, *J* = 8.2 Hz), 7.79 (d, 2H, *J* = 8.6 Hz), 7.74-7.63 (m, 2H), 7.23 (d, 2H, *J* = 8.6 Hz), 5.10-5.02 (m, 1H), 4.11-4.02 (m, 2H), 3.58 (s, 2H), 1.88-1.73 (m, 2H), 1.69-1.46 (m, 6H). MS, *m/z*: 567.15 $(M + H)^+$.

Tetrahydro-2*H*-pyran-3-yl (4-{[(2'-(aminomethyl)-5'-{[(3-fluoropyridin-4-yl)amino]carbonyl}biphenyl-3-yl)carbonyl]amino}phenyl)acetate, TFA salt (29)

^{1}H NMR (DMSO-*d6*, 400 MHz): δ 10.67 (s, 1H), 10.34 (s, 1H), 8.63 (d, 1H, *J* = 2.7 Hz), 8.42 (d, 1H, *J* = 5.3 Hz), 8.31 (br s, 3H), 8.12 (dd, 1H, *J* = 8.2, 1.9 Hz), 8.09-8.06 (m, 1H), 8.05-8.04 (m, 1H), 8.03 (d, 1H, *J* = 1.9), 7.93 (dd, 1H, *J* = 6.6, 5.4 Hz), 7.81 (d, 1H, *J* = 8.2 Hz), 7.73 (d, 2H, *J* = 8.6 Hz), 7.71-7.67 (m, 2H), 7.26 (d, 2H, *J* = 8.6 Hz), 4.71-4.64 (m, 1H), 4.09 (q, 2H, *J* = 5.7 Hz), 3.70-3.62 (m, 3H), 3.54 (t, 2H, *J* = 5.2 Hz), 3.44 (dd, 1H, *J* = 11.6, 5.7 Hz), 1.94-1.80 (m, 1H), 1.77-1.57 (m, 2H), 1.53-1.41 (m, 1H). MS, *m/z*: 582.99 $(M + H)^+$.

1-Methylpiperidin-4-yl (4-{[(2'-(aminomethyl)-5'-{[(3-fluoropyridin-4-yl)amino]carbonyl}biphenyl-3-yl)carbonyl]amino}phenyl)acetate, TFA salt (30)

2 conformational isomers (see supporting information, for a graphical representation).

^{1}H NMR (DMSO-*d6*, 300 MHz): δ 10.69 (s, 1H), 10.37 (d, 1H, *J* = 2.4 Hz), 9.77 (br s, 1H), 9.63 (d, 1H, *J* = 2.7 Hz), 8.50-8.25 (m, 3H), 8.42 (d, 1H, *J* = 5.3 Hz), 8.12 (dd, 1H, *J* = 8.2, 1.8 Hz), 8.10-8.00 (m, 3H), 7.92 (dd, 1H, *J* = 6.6, 5.5 Hz), 7.82 (d, 1H, *J* = 8.2 Hz), 7.78-7.67 (m, 4H),

7.35-7.21 (m, 2H), 5.02-4.94 (m, 0.5H), 4.92-4.76 (m, 0.5H), 4.15-4.02 (m, 2H), 3.69 (s, 1H), 3.66 (s, 1H), 3.52-3.26 (m, 2H), 3.18-2.90 (m, 2H), 2.75-2.70 (m, 3H), 2.17-2.05 (m, 1H), 2.01-1.84 (m, 2H), 1.82-1.62 (m, 1H). MS, *m/z*: 596.19 $(M + H)^+$.

Propyl 4-{[(2'-(aminomethyl)-5'-{[(3-fluoropyridin-4-yl)amino]carbonyl}biphenyl-3-yl)carbonyl]amino}benzoate, TFA salt (31)

^{1}H NMR (DMSO-*d6*, 300 MHz): δ 10.69 (s, 1H), 10.67 (s, 1H), 8.64 (d, 1H, *J* = 2.7 Hz), 8.42 (d, 1H, *J* = 5.3 Hz), 8.40-8.26 (m, 3H), 8.17-7.89 (m, 9H), 7.82 (d, 1H, *J* = 8.2 Hz), 7.76-7.68 (m, 2H), 4.21 (t, 2H, *J* = 6.5 Hz), 4.09 (q, 2H, *J* = 5.6 Hz), 1.80-1.64 (m, 2H), 0.97 (t, 3H, *J* = 7.4 Hz). MS, *m/z*: 527.09 $(M + H)^+$.

Methyl 4-{[(2'-(aminomethyl)-5'-{[(3-fluoropyridin-4-yl)amino]carbonyl}biphenyl-3-yl)amino]carbonyl}benzoate, TFA salt (32)

^{1}H NMR (DMSO-*d6*, 300 MHz): δ 10.68 (s, 1H), 10.64 (s, 1H), 8.64 (d, 1H, *J* = 2.8 Hz), 8.42 (d, 1H, *J* = 5.4 Hz), 8.40-8.26 (m, 3H), 8.16-8.05 (m, 5H), 7.99 (d, 1H, *J* = 1.8 Hz), 7.97-7.90 (m, 2H), 7.87-7.76 (m, 2H), 7.54 (t, 1H, *J* = 7.9 Hz), 7.28-7.21 (m, 1H), 4.13 (q, 2H, J = 5.6 Hz), 3.40 (s, 3H). MS, *m/z*: 499.07 $(M + H)^+$.

3-{[(2'-(Aminomethyl)-5'-{[(3-fluoropyridin-4-yl)amino]carbonyl}biphenyl-3-yl)carbonyl]amino}benzoic acid, TFA salt (6M)

^{1}H NMR (DMSO-*d6*, 400 MHz): δ 10.68 (s, 1H), 10.53 (s, 1H), 8.63 (d, 1H, *J* = 2.8 Hz), 8.45-8.39 (m, 2H), 8.39-8.22 (m, 3H), 8.16-8.05 (m, 4H), 8.04 (d, 1H, *J* = 1.9 Hz), 7.93 (dd, 1H, *J* = 5.4, 6.7 Hz), 7.81 (d, 1H, *J* = 8.2 Hz), 7.75-7.65 (m, 3H), 7.50 (t, 1H, *J* = 8.0 Hz), 4.14-4.04 (m, 2H). MS, *m/z*: 485.13 $(M + H)^+$.

(3-{[(2'-(Aminomethyl)-5'-{[(3-fluoropyridin-4-yl)amino]carbonyl}biphenyl-3-yl)carbonyl]amino}phenyl)acetic acid, HCl salt (7M)

^{1}H NMR (DMSO-*d6*, 400 MHz): δ 10.68 (s, 1H), 10.42 (s, 1H), 8.73 (s, 1H), 8.52 (br s, 3H), 8.48 (d, 1H, J = 5.5 Hz), 8.15-8.03 (m, 5H), 7.88 (d, 1H, J = 8.2 Hz), 7.75-7.66 (m, 4H), 7.29 (t, 1H, J = 7.8 Hz), 7.01 (d, 1H, J = 7.6 Hz), 4.08 (d, 2H, J = 5.6 Hz), 3.56 (s, 2H). MS, *m/z*: 499.20 $(M + H)^+$.

4-{[(2'-(Aminomethyl)-5'-{[(3-fluoropyridin-4-yl)amino]carbonyl}biphenyl-3-yl)carbonyl]amino}benzoic acid, HCl salt (8M)

^{1}H NMR (DMSO-*d6*, 300 MHz): δ 11.24 (s, 1H), 10.83 (s, 1H), 8.82-8.63 (m, 3H), 8.59 (d, 1H, *J* = 6.0 Hz), 8.32 (t, 1H, *J* = 6.5 Hz), 8.27-8.22 (m, 1H), 8.16-8.06 (m, 3H), 8.06-7.98 (m, 2H), 7.98-7.87 (m, 3H), 7.79-7.62 (m, 3H), 4.18-3.96 (m, 2H). MS, *m/z*: 485.10 $(M + H)^+$.

(4-{[(2'-(Aminomethyl)-5'-{[(3-fluoropyridin-4-yl)amino]carbonyl}biphenyl-3-yl)carbonyl]amino}phenyl)acetic acid (9M)

^{1}H NMR (DMSO-*d6*, 400 MHz): δ 10.54 (br s, 1H), 10.30 (s, 1H), 8.59 (d, 1H, *J* = 2.7 Hz), 8.39 (d, 1H, *J* = 5.3 Hz), 8.07-7.98 (m, 3H), 7.93 (d, 1H, *J* = 1.9 Hz), 7.90 (dd, 1H, *J* = 6.7, 5.4 Hz), 7.82 (d, 1H, *J* = 8.1 Hz), 7.74-7.61 (m, 4H), 7.26-7.17 (m, 2H), 3.76 (s, 2H), 3.49 (s, 2H). MS, *m/z*: 499.04 $(M + H)^+$.

3-{[(2'-(Aminomethyl)-5'-{[(3-fluoropyridin-4-yl)amino]carbonyl}biphenyl-3-yl)carbonyl]amino}-4-fluorobenzoic acid, TFA salt (13M)

^{1}H NMR (DMSO-*d6*, 300 MHz): δ 10.70 (s, 1H), 10.41 (s, 1H), 8.64 (d, 1H, *J* = 2.7 Hz), 8.43 (d, 1H, *J* = 5.4 Hz), 8.39-8.20 (m, 3H), 8.23 (dd, 1H, *J* = 7.5, 2.1 Hz), 8.16-8.05 (m, 3H), 8.03 (d,

1H, *J* = 1.7 Hz), 7.95 (dd, 1H, *J* = 6.5, 5.8 Hz), 7.91-7.82 (ddd, 1H, *J* = 8.6, 4.8, 2.2 Hz), 7.81 (d, 1H, *J* = 8.2 Hz), 7.77-7.66 (m, 2H), 7.44 (dd, 1H, *J* = 10.1, 8.3 Hz), 4.20-4.02 (m, 2H). MS, *m/z*: 503.12 $(M + H)^+$.

3-{[(2'-(Aminomethyl)-5'-{[(3-fluoropyridin-4-yl)amino]carbonyl}biphenyl-3-yl)amino]carbonyl}benzoic acid, HCl salt (17M)

^{1}H NMR (DMSO-*d6*, 400 MHz): δ 10.75 (s, 1H), 10.68 (s, 1H), 8.66 (d, 1H, *J* = 2.3 Hz), 8.63-8.49 (m, 4H), 8.43 (d, 1H, *J* = 5.4 Hz), 8.25 (d, 1H, *J* = 7.8 Hz), 8.15 (d, 1H, *J* = 7.7 Hz), 8.10 (dd, 1H, *J* = 8.14, 1.5 Hz), 8.02-7.95 (m, 2H), 7.93 (s, 1H), 7.89 (d, 2H, *J* = 8.2 Hz), 7.68 (t, 1H, *J* = 7.7 Hz), 7.53 (t, 1H, *J* = 7.9 Hz), 7.29-7.21(m, 1H), 4.17-4.04 (m, 2H). MS, *m/z*: 485.06 $(M + H)^+$.

3-{[(2'-(Aminomethyl)-5'-{[(3-fluoropyridin-4-yl)amino]carbonyl}biphenyl-3-yl)amino]carbonyl}-4-fluorobenzoic acid, TFA salt (19M)

Due to limited commercial availability of 2-fluoro-5-(methoxycarbonyl)benzoic acid, compound **19M** was not synthesized using the general scheme and methods. For the synthetic route and protocols, we refer to the Supporting Information.

^{1}H NMR (DMSO-*d6*, 400 MHz): δ 10.74 (s, 1H), 10.66 (s, 1H), 8.63 (d, 1H, *J* = 2.7 Hz), 8.41 (d, 1H, *J* = 5.3 Hz), 8.39-8.26 (m, 3H), 8.22 (dd, 1H, *J* = 6.8, 2.2 Hz), 8.17-8.11 (m, 1H), 8.11 (dd, 1H, *J* = 8.2, 1.9 Hz), 7.99 (d, 1H, *J* = 1.8 Hz), 7.92 (dd, 1H, *J* = 6.6, 5.5 Hz), 7.90-7.85 (m, 1H), 7.80 (d, 1H, *J* = 8.2 Hz), 7.77-7.70 (m, 1H), 7.58-7.46 (m, 2H), 7.29-7.20 (m, 1H), 4.18-4.04 (m, 2H). MS, *m/z*: 503.09 $(M + H)^+$.

3-{[(2'-(Aminomethyl)-5'-{[(3-fluoropyridin-4-yl)amino]carbonyl}biphenyl-3-yl)carbonyl]amino}-2-fluorobenzoic acid, HCl salt (21M)

^{1}H NMR (DMSO-*d6*, 400 MHz): δ 11.04 (s, 1H), 10.49 (s, 1H), 8.84 (s, 1H), 8.64 (br s, 3H), 8.53 (d, 1H, J = 5.5 Hz), 8.23-8.03 (m, 5H), 7.93 (d, 1H, J = 8.13 Hz), 7.81 (t, 1H, J = 7.2 Hz), 7.79-7.65 (m, 3H), 7.32 (t, 1H, J = 7.8 Hz), 4.08 (d, 2H, J = 4.9 Hz). MS, *m/z*: 503.20 $(M + H)^+$.

4-{[(2'-(Aminomethyl)-5'-{[(3-fluoropyridin-4-yl)amino]carbonyl}biphenyl-3-yl)amino]carbonyl}benzoic acid, HCl salt (32M)

^{1}H NMR (DMSO-*d6*, 300 MHz): δ 10.81 (s, 1H), 10.67 (s, 1H), 8.71 (d, 1H, *J* = 2.4 Hz), 8.65-8.50 (m, 3H), 8.46 (d, 1H, *J* = 5.4 Hz), 8.19-7.92 (m, 8H), 7.92-7.83 (m, 2H), 7.53 (t, 1H, *J* = 7.9 Hz), 7.31-7.20 (m, 1H), 4.18-4.02 (m, 2H). MS, *m/z*: 485.10 $(M + H)^+$.

Biological assays:

Kinase inhibition

Kinase inhibition data was measured externally at Reactions Biology Corporation (Malvern, USA) in a radiometric assay. For ROCK1 and ROCK 2 IC_{50} determination, the competing ATP concentration was 1μM (initial screen) or 200μM (secondary assay for the most active compounds). The formal enzyme concentration was 1nM in both cases.

Kinase selectivity data was collected externally at Reactions Biology Corporation (Malvern, USA) in a radiometric assay, against a panel of 335 kinases. The competing ATP concentration was 10μM.

Further details regarding the assay technology can be obtained in literature. (Anastassiadis, T.; Deacon, S. W.; Devarajan, K.; Ma, H.; Peterson, J. R. *Nat Biotechnol.* **2011**, 29(11), 1039)

MLC phosphorylation

MLC phosphorylation data was generated at Proqinase GmbH (Freiburg, Germany), by implementing the MLC phosphorylation assay initially described by Schröter *et al.*[24] The rat smooth muscle cell line A7r5 was used. Endogenous expression of ROCK in those cells results in a constitutive phosphorylation of the regulatory myosin light chain at T18/S19. A7r5 cells were plated in DMEM supplemented with 10% FCS in multiwell cell culture plates. Next day, medium was exchanged for serum-free medium and compounds were added. Cells were incubated for 90 min after addition of the compounds. Quantification of MLC-Thr18/Ser19 phosphorylation was then assessed *via* ELISA, using a phospho-MLC-Thr18/Ser19 specific antibody and a secondary detection antibody. Cells treated with 100µM Y-27362 were defined as low control (0%), while cells treated with vehicle were defined as high control (100%). For inhibitors, raw data were converted into percent substrate phosphorylation relative to high control. IC_{50} values were determined using GraphPad Prism 5 software with constrain of bottom to 0 and top to 100 using a nonlinear regression curve fit with variable hill slope four-parameter logistic equation).

Compound stability in plasma

Pooled, mixed gender, heparinised human plasma was purchased from Sera Laboratories International (Haywards Heath, UK). Plasma samples (195µl) were spiked with 5µl test compounds provided as 10mM DMSO stock (final DMSO concentration 0.2%). The resulting mixtures were stirred (300rpm) and incubated at 37°C for 60 min. Samples were taken at fixed time points and put into ice-cold acetonitrile containing the internal standard metoprolol (Sigma Aldrich, Steinheim, Germany) for protein precipitation. The remnant of compound was determined by LC-MS/MS (LC20AD, Shimadzu, Duisburg, Germany, 3200 Q TRAP

LC/MS/MS system, AB Applied Biosystems, MSD Sciex, Niewenkerk aan den Ijssel, The Netherlands) using Analyst Software (AB Sciex). The $t_{1/2}$ values were then determined with GraphPad Prism 5.01 software, assuming one phase decay.

For inhibition studies, the following esterase inhibitors were added at the following final concentrations:

- Disodium EDTA (Sigma Aldrich, Steinheim, Germany): 5mM
- Tacrine (Sigma Aldrich, Steinheim, Germany): 10µM
- PMSF (Phenylmethylsulfonyl fluoride) (Sigma Aldrich, Steinheim, Germany) : 250µM
- BNPP (Bis-4-nitrophenyl phosphate) (Sigma Aldrich, Steinheim, Germany): 50µM

HDF-1 cell culture

The human dermal fibroblasts (HDF-1) were purchased from Sigma -Aldrich (St-Louis, MO) and cultured in complete fibroblast growth medium (Sigma–Aldrich) supplemented with 2% heat-inactivated fetal calf serum (FCS; Sigma-Aldrich) in CellBind culture flasks (Sigma-Aldrich, St Louis, MO). Cells were subcultured 1:10.

HDF-1 cell viability

HDF-1 were seeded in 96 well plate at a density of 75000cells/ml in complete fibroblast growth medium (Sigma-Aldrich) and allowed to adhere for 24h. Cells were subsequently exposed to different concentrations (0.01-100µM) of the ROCK inhibitors for another 24h after which the viability was determined using the colorimetric cell proliferation reagent WST-1 (Roche, Mannheim, Germany). DMSO controls corresponding to vehicle were included for all

concentrations. At least 3 independent experiments were performed. In each experiment, measurements were done in triplicate.

HDF-1 apoptosis

HDF-1 cells were plated in 96-well culture plates at a density of 75000cell/ml and allowed to attach for 24h in complete fibroblast growth medium (Sigma-Aldrich). Next, cells were incubated for 24h in presence of different concentration of ROCK inhibitors. Apoptosis was analyzed by measuring the caspase-3/7 activity with the Caspase-Glo 3/7 assay (Promega Corp., Madison, WI) according to the manufacturer's instructions. DMSO controls corresponding to vehicle were included for all concentrations. At least 3 independent experiments were performed. In each experiment, measurements were done in triplicate.

HDF-1 cell migration measurements

Migration HDF-1 was measured using the wound assay. 20000 HDF-1 cells were cultured to a confluent monolayer in complete fibroblast growth medium (Sigma-Aldrich) in 48-well culture plates. Using a sterile 20-µl pipette tip, a wound was made in the well. Wounded monolayers were washed with PBS to remove non-adherent cells. Next, cells were treated with the different ROCK inhibitors for 8 h. Wound width was measured at 4 locations predefined at start and at 2, 4, 6, and 8 hours after wounding. The rate of cell migration is inversely correlated to the wound width. All experiments were performed at least in triplicate.

Caco2 permeability

Caco2 permeability was determined externally at Cerep SA (now Eurofins Cerep SA, Celle l'Evescault, France).

Compound stability vs. Hepatocytes

Stability of **8** in presence of hepatocytes was studied externally at Notox BV (now WIL Research BV, The Netherlands).

Human (2 donors) and rabbit (New Zealand White) hepatocytes were thawed according to the WIL Research Europe standard operating procedures. The number of hepatocytes was determined using an "Improved Neubauer" haemocytometer.

Viability of the hepatocytes was determined using the Trypan blue dye exclusion method, by mixing 25 µL or 50 µL of the hepatocyte suspension with an equal volume of 0.4 % trypan blue dye solution and by counting the viable (colorless) and non-viable (blue-colored) hepatocytes. The hepatocyte viability was defined as the percentage of viable cells. Only hepatocytes with a viability ≥ 70% were used.

Duplicate incubation mixtures with **8** (1 µM and 10 µM final concentration) and single incubation mixtures with vehicle were prepared in glass vials closed with a screw cap. Phosphate-buffered saline (PBS) was used as incubation buffer. The final concentration of hepatocytes was 1 x 10^6 cells /mL. Each incubation mixture was divided into five vials of 200 µL each and one vial with the remaining mixture for determination of the hepatocyte viability after 120±1 minutes of incubation. Vials were incubated in a shaking water bath at 37°C. At 1±1, 30 ± 1, 60 ± 1, 90 ± 1 and 120 ± 1 minutes incubation vials were cooled down on ice and 100 µL acetonitrile was added. After vortex-mixing the samples were centrifuged for 5 min at 16000 g, and subjected to LC-PDA-MS analysis.

Rabbit Pharmacokinetics

Male New Zealand White rabbits received a single intravenous injection of **8** (0.1 mg/kg). Blood samples were collected 1, 5, 10, 15, 20, 30, 60, 120, 240 and 360 min after administration. Samples were processed to plasma and stored at -20°C until analysis. Plasma samples were extracted by acetonitrile precipitation. Individual and average plasma concentrations for both **8** and **8M** were determined by LC-MS/MS (LC20AD, Shimadzu, Duisburg, Germany, 3200 Q TRAP LC/MS/MS system, AB Applied Biosystems, MSD Sciex, Niewenkerk aan den Ijssel, The Netherlands) using Analyst Software (AB Sciex). 10-point calibration curves were prepared for **8** and **8M** at concentrations ranging from 0.4-900 nM in the injected sample (corresponding to 4-9000 nM in the unprocessed plasma sample) by serial dilution. The limit of quantitation (plasma sample) was 8nM for **8 and** 35 nM for **8M.** Concentrations were reported as average ± SEM, in nanomolar (nM) units. Data points collected between 10min and last point above LOQ (60 min for **8** and 120 min for **8M**) were used for estimating plasma half life ($t_{1/2}$), which was calculated from 0.693/slope (one phase decay).

Crystal structure determination

Crystal structure determination was handled externally at Proteros GmbH (Planegg-Martinsried, Germany). Suitable constructs for ROCK2 expression had been previously established by Proteros. Expression and purification of ROCK2 was performed according to previously established protocols. The purified protein was used in crystallization trials employing both a standard screen with approximately 1200 different conditions, as well as crystallization conditions identified using literature data. Conditions initially obtained were further refined.

ROCK2 crystals were ultimately grown by vapor diffusion (hanging drop) method at 20°C, pH 6.3, using PEG as precipitant.

The X-ray diffraction data was collected from complex crystals of ROCK2 with compound 10 at the Swiss Light Source (SLS, Villigen, Switzerland) using cryogenic (100 K) conditions. XRD data could be collected to a resolution of 2.93Å. Crystals belonged to space group C 2. Data were processed using the programs XDS and XSCALE. The phase information necessary to determine and analyze the structure was obtained by molecular replacement. A previously solved structure of ROCK2 was used as a search model. Subsequent model building and refinement was performed according to standard protocols with the software packages CCP4 and COOT. TLS refinement (using REFMAC5, CCP4) has been carried out, which resulted in lower R-factors and higher quality of the electron density map. The Ramachandran Plot of the final model shows 89.6 % of all residues in the most favored region, 10.0 % in the additionally allowed region, and 0.4 % in the generously allowed region. No residues are found in the disallowed region.

The interpreted X-ray diffraction data essentially showed a clear binding mode, as well as the orientation and conformation of the ligand bound to the active site. However B-factors were the highest for methyl ester moiety of the bound ligand. As position of the final carbon atom could not be clearly defined, its occupancy was set to 0 in all monomers present in the asymmetric unit. This carbon atom was nonetheless kept in the model so not to create confusion with the carboxylic acid analog of the bound ligand.

The final model was deposited in the PDB (www.rcsb.org) under entry code 4WOT.

ASSOCIATED CONTENT

Supporting Information. Alternative scheme for synthesis of **19**, **20**, and **19M**; additional scheme for conformational isomers of **30; PK** curves for compound **8**; numerical selectivity data for **8**. This material is available free of charge via the Internet at http://pubs.acs.org.

PDB ID CODES

4WOT

AUTHOR INFORMATION

Corresponding Author

Sandro Boland, Ph.D.

Amakem N.V. Agoralaan Abis, 3590 Diepenbeek. Belgium.

+32 (0)11 286973

sandro.boland@amakem.com

Author Contributions

The manuscript was written through contributions of all authors. All authors have given approval to the final version of the manuscript.

ACKNOWLEDGMENTS

The authors wish to acknowledge the Proteros team, including Dr. Martin Augustin, Dr. Stephan Krapp, Dr Stefan Steinbacher and Dr Lars Hesse for their work on the ROCK2 crystal structure and their help in the preparation of the manuscript. The authors also wish to thank Prof. Nicolas Willand (Université Lille 2, Lille, France), Dr. Jack Elands and Dr. Steve Pakola (Amakem Therapeutics) for critical reading of the manuscript.

ABBREVIATIONS

AGC, protein kinase A G and C family; AMD, age-related macular degeneration; ATP, Adenosine triphosphate; BNPP, bis-4-nitrophenylphosphate; CC_{50}, Cytotoxic concentration 50; CES1, carboxylesterase 1; CES2, carboxylesterase 2; DTNB, 5,5'-dithiobis-(2-nitrobenzoic acid); EC_{50}, effective concentration 50 (cell-based assays); EDTA, ethylenediaminetetraacetic acid; HDF, human dermal fibroblast; IC_{50}, inhibitory concentration 50 (on-target assays); IOP, intraocular pressure; MLC, Myosin Light Chain; MLC-PP, Myosin light chain phosphorylation; NZW rabbit, New Zealand White rabbit; PAH, pulmonary arterial hypertension; PMSF, phenylmethylsulfonyl fluoride; PON1, paraoxonase 1; ROCK, Rho-associated, coiled coil containing protein kinase; TPSA, topological polar surface area.

REFERENCES

1. Matsui, T.; Amano, M.; Yamamoto, T.; Chihara, K.; Nakafuku, M.; Ito, M.; Nakano, T.; Okawa, K.; Iwamatsu, A.; Kaibuchi, K. Rho-associated kinase, a novel serine/threonine kinase, as a putative target for small GTP binding protein Rho. *EMBO J.* **1996**, *15*, 2208–2216.

2. Riento, K.; Ridley, A. J. ROCKS: multifunctional kinases in cell behavior. *Nat. Rev. Mol. Cell Biol.* **2003**, *4*, 446-456.

3. Liao, J. K.; Seto, M.; Noma, K. Rho kinase (ROCK) inhibitors. *J. Cardiovasc. Pharmacol.* **2007**, *50*, 17-24.

4. Antoniu, S. A. Targeting RhoA/ROCK pathway in pulmonary arterial hypertension. *Expert Opin. Ther. Targets*. **2012**, *16*, 355-63.

5. LoGrasso, P. V.; Feng, Y. Rho kinase (ROCK) inhibitors and their application to inflammatory disorders. *Curr. Top. Med. Chem.* **2009**, *9(8)*, 704-723.

6. Doe, C.; Bentley, R.; Behm, D. J.; Lafferty, R.; Stavenger, R.; Jung, D.; Bamford, M.; Panchal, T.; Grygielko, E.; Wright, L. L.; Smith, G. K.; Chen, Z.; Webb, C.; Khandekar, S.; Yi, T. Novel Rho kinase inhibitors with anti-inflammatory and vasodilatory activities. *J. Pharmacol. Exp. Ther.* **2007**, *320(1)*, 89-98.

7. Fernandes, L. B.; Henry, P. J.; Goldie, R. G. Rho kinase as a therapeutic target in the treatment of asthma and chronic obstructive pulmonary disease. *Ther. Adv. Respir. Dis.* **2007,** *1*, 25-33.

8. Mandell, K. J.; Kudelka, M. R.; Wirostko, B. Rho kinase inhibitors for treatment of glaucoma. *Expert Rev. Ophthalmol.* **2011**, *6(6)*, 611-622.

9. Fukumoto, Y.; Yamada, N.; Matsubara, H.; Mizoguchi, M.; Uchino, K.; Yao, A.; Kihara, Y.; Kawano, M.; Watanabe, H.; Takeda, Y.; Adachi, T.; Osanai, S.; Tanabe, N.; Inoue, T.; Kubo, A.; Ota, Y.; Fukuda, K.; Nakano, T.; Shimokawa, H. Double-blind, placebo-controlled clinical trial with a rho-kinase inhibitor in pulmonary arterial hypertension. *Circ. J.* **2013**, *77*, 2619-2625.

10. Kast, R.; Schirok, H.; Figueroa-Pérez, S.; Mittendorf, J.; Gnoth, M. J.; Apeler, H.; Lenz, J.; Franz, J. K.; Knorr, A.; Hütter, J.; Lobell, M.; Zimmermann, K.; Münter, K.; Augstein, K. H.; Ehmke, H.; Stasch, J. P. Cardiovascular effects of a novel potent and highly selective azaindole-based inhibitor of Rho-kinase. *Br. J. Pharmacol.* **2007**, *152(7)*, 1070-1080.

11. Shaw, D.; Hollingworth, G.; Soldermann, N.; Sprague, E.; Schuler, W.; Vangrevelinghe, E.; Duggan, N.; Thomas, M.; Kosaka, T.; Waters, N.; van Eis, M. J. Novel ROCK inhibitors for the treatment of pulmonary arterial hypertension. *Bioorg. Med. Chem. Lett.* **2014**, *24*, 4812-4817.

12. Isobe, T.; Mizuno, K.; Kaneko, Y.; Ohta, M.; Koide, T.; Tanabe, S. Effects of K-115, a Rho-Kinase Inhibiror, on Aqueous Humor Dynamics in Rabbits. *Curr. Eye Res.* **2014**, *39*, 813-822.

13. Okumura, N.; Koizumi, N.; Kay, E. P.; Ueno, M.; Sakamoto, Y.; Nakamura, S.; Hamuro, J.; Kinoshita, S. The ROCK inhibitor eye drop accelerates corneal endothelium wound healing. *Invest. Ophthalmol. Vis. Sci.* **2013**, *54*, 2493-2502.

14. Koizumi, N.; Okumura, N.; Ueno, M.; Nakagawa, H.; Hamuro, J.; Kinoshita, S. Rho-associated kinase inhibitor eye drop treatment as a possible medical treatment for Fuchs corneal dystrophy. *Cornea.* **2013**, *32*, 1167-1170.

15. Koizumi, N.; Okumura, N.; Ueno, M.; Kinoshita, S. New therapeutic modality for corneal endothelial disease using rho-associated kinase inhibitor eye drops. *Cornea*, **2014**, *33*, Suppl. 11, S25-31

16. Tokushige, H.; Inatani, M.; Nemoto, S.; Sakaki, H.; Katayama, K.; Uehata, M; Tanihara, H. Effects of topical administration of Y-39983, a selective rho-associated protein kinase inhibitor, on ocular tissues in rabbits and monkeys. *Invest. Ophthalmol. Vis. Sci.* **2007,** *48,* 3216-3222.

17. Tanihara, H.; Inatani, M. ; Honjo, M.; Tokushige, H. ; Azuma, J. ; Araie, M. Intraocular pressure-lowering effects and safety of topical administration of a selective ROCK inhibitor, SNJ-1656, in healthy volunteers. *Arch. Ophthalmol.* **2008**, *126(3)*, 309-315.

18. Bodor, N.; Buchwald, P. Retrometabolism-based drug design and targeting. In *Burger's Medicinal Chemistry and Drug Discovery*, Vol. 2, *Drug Discovery and Drug Development*, 6th ed.; Abraham, D. J., Ed.; Wiley: Hoboken, 2003; pp 533-608.

19. Erhardt, P. W.; Reese, M. D. In *Prodrugs and Targeted Delivery: Towards Better ADME Properties.* (ed. J. Rautio), Wiley-VCH Verlag GmbH & Co.: Weinheim, 2011; pp. 385-413.

20. Boland, S.; Defert, O.; Alen, J.; Bourin, A.; Castermans, K.; Kindt, N.; Boumans, N.; Panitti, L.; Van de Velde, S.; Stalmans, I.; Leysen, D. 3-[2-(Aminomethyl)-5-[(pyridin-4-yl)carbamoyl]phenyl] benzoates as soft ROCK inhibitors. *Bioorg. Med. Chem. Lett.* **2013**, *23*, 6442-6446.

21. Van de Velde, S.; Van Bergen, T.; Sijnave, D.; Hollanders, K.; Castermans, K.; Defert, O.; Leysen, D.; Vandewalle, E.; Moons, L.; Stalmans, I. AMA0076, a novel, locally acting Rho kinase inhibitor, potently lowers intraocular pressure in New Zealand white rabbits with minimal hyperemia. *Invest. Ophthalmol. Vis. Sci.* **2014**, *55*, 1006-1016.

22. Jacobs, M.; Hayakawa, K.; Swenson, L.; Bellon, S.; Fleming, M.; Taslimi, P.; Doran, J. The structure of dimeric ROCK I reveals the mechanism for ligand selectivity. *J. Biol. Chem.* **2006,** *281*, 260-268.

23. Anastassiadis, T.; Deacon, S.W.; Devarajan, K.; Ma, H.; Peterson, J. R. Comprehensive assay of kinase catalytic activity reveals features of kinase inhibitor selectivity. *Nat. Biotechnol.* **2011**, *29*, 1039-1045.

24. Schröter, T.; Griffin, E.; Weiser, A.; Feng, Y.; LoGrasso, P. Detection of myosin light chain phosphorylation--a cell-based assay for screening Rho-kinase inhibitors. *Biochem. Biophys. Res. Commun.* **2008**, *374(2)*, 356-360.

25. Gleeson, M. P. Generation of a set of simple, interpretable ADMET rules of thumb. *J. Med. Chem.* **2008**, *51(4)*, 817-834.

26. Hasan, F. B.; Cohen, S. G.; Cohen, J. B. Hydrolysis by acetylcholinesterase. Apparent molal volumes and trimethyl and methyl subsites. *J. Biol. Chem.* **1980**, *255*, 3898-3904.

27. Li, B.; Sedlacek, M.; Manoharan, I.; Boopathy, R.; Duysen, E. G.; Masson, P.; Lockridge, O. Butyrylcholinesterase, paraoxonase, and albumin esterase, but not carboxylesterase, are present in human plasma. *Biochem. Pharmacol.* **2005**, *70*, 1673-1684.

28. Khersonsky, O.; Tawfik, D. S. Structure-reactivity studies of serum paraoxonase PON1 suggest that its native activity is lactonase. *Biochemistry* **2005**, *44*, 6371-6382.

29. Karaman, M. W.; Herrgard, S.; Treiber, D. K.; Gallant, P.; Atteridge, C. E.; Campbell, B. T.; Chan, K. W.; Ciceri, P.; Davis, M. I.; Edeen, P. T.; Faraoni, R.; Floyd, M.; Hunt, J. P.; Lockhart, D. J.; Milanov, Z. V.; Morrison, M. J.; Pallares, G.; Patel, H. K.; Pritchard, S.; Wodicka, L. M.; Zarrinkar, P. P. A quantitative analysis of kinase inhibitor selectivity. *Nat. Biotechnol.* **2008**, *26*, 127-132.

30. Darenfed, H.; Dayanandan, B.; Zhang, T.; Hsieh, S. H.; Fournier, A.E.; Mandato, C. A. Molecular characterization of the effects of Y-27632. *Cell Motil. Cytoskeleton.* **2007**, *64*, 97-109.

31. Kim, S. J.; Kim, J. H.; Sun, J. M.; Kim, M. G.; Oh, J. W. Suppression of hepatitis C virus replication by protein kinase C-related kinase 2 inhibitors that block phosphorylation of viral RNA polymerase. *J. Viral Hepat.* **2009***, 16*, 697-704.

32. Honjo, M.; Tanihara, H.; Kameda, T.; Kawaji, T.; Yoshimura, N.; Araie, M. Potential role of Rho-associated protein kinase inhibitor Y-27632 in glaucoma filtration surgery. *Invest. Ophthalmol. Vis. Sci.* **2007**, *48*, 5549-5557.

33. Castermans, K.; Tabruyn, S. P.; Zeng, R.; van Beijnum, J. R.; Eppolito, C.; Leonard, W. J.; Shrikant, P. A.; Griffioen, A. W. Angiostatic activity of the antitumor cytokine interleukin-21. *Blood*. **2008**, *112*, 4940-4947.

34. Sijnave, D.; Van Bergen, T.; Castermans, K.; Kindt, N.; Vandewalle, E.; Stassen, J. M.; Moons, L.; Stalmans, I. Inhibition of rho-associated kinase prevents pathological wound healing and neovascularization after corneal trauma. *Cornea.* **2015,** (Paper submitted).

35. Hollanders, K.; Van Bergen, T.; Kindt, N.; Castermans, K.; Leysen, D.; Vandewalle, E.; Moons, L.; Stalmans, I. The effect of AMA0428, a novel and potent ROCK inhibitor, in a model of neovascular age-related macular degeneration. *Invest. Ophthalmol. Vis. Sci.* **2015**, *56*, 1335-1348.

36. Imai, T.; Taketani, M.; Shii, M.; Hosokawa, M.; Chiba, K. Substrate specificity of carboxylesterase isozymes and their contribution to hydrolase activity in human liver and small intestine. *Drug Metab. Dispos.* **2006**, *34*, 1734-1741.

37. Satoh, T.; Hosokawa, M. Carboxylesterases: structure, function and polymorphism in mammals. *J. Pestic. Sci.* **2010**, *35*, 218-228.